

## ABSTRACT

Title of Document:

BEAM INJECTION AND MATCHING  
STUDIES IN THE UNIVERSITY OF  
MARYLAND ELECTRON RING

Jayakar Charles Tobin Thangaraj, Master of  
Science, 2006

Directed By:

Professor Patrick O'Shea  
Department of Electrical and Computer  
Engineering

Intense charged particle beams are of great interest to many wide areas of applications ranging from high-energy physics to free-electron lasers. The University of Maryland Electron Ring (UMER) is a scaled model to investigate the physics of such intense beams. Recently, multi turn operation of the ring (3.6 m diameter) has begun. In order to have full current transport of the electron beam, and to increase the number of turns of the beam around the ring, injection and matching of the beam from the straight section into the ring becomes crucial. Injection is done through a quadrupole fringe field, making it more challenging. Careful injection of a matched beam will also minimize emittance growth and halo formation around the ring. In this thesis, experimental results from the injection, matching, and transport of a space charge dominated beam and an emittance dominated beam are reported.

BEAM INJECTION AND MATCHING STUDIES IN THE UNIVERSITY OF  
MARYLAND ELECTRON RING.

By

Jayakar Charles Tobin Thangaraj

Thesis submitted to the Faculty of the Graduate School of the  
University of Maryland, College Park, in partial fulfillment  
of the requirements for the degree of  
Master of Science  
2006

Advisory Committee:  
Professor Patrick O'Shea, Chair/Advisor  
Professor Emeritus Martin Reiser  
Professor Rami A.Kishek

© Copyright by  
Jayakar Charles Tobin Thangaraj  
2006

## Dedication

To my parents and younger brother,

Joshua Daniel Thangaraj,

Beulah Thangaraj ,

Jeromie Wesley Vivian

## Acknowledgements

First and foremost, I would like to thank my advisor, Professor Patrick O'Shea for his guidance for the successful completion of my thesis. His broad knowledge in beam physics and professional expertise coupled with his cheerful disposition has made my life in graduate school an enjoyable one. In spite of handling a busy job of leading one of the biggest departments in the university, he took time for his graduate students and their career. I would like to thank Professor Martin Reiser, for his valuable advice and invaluable book. I would like to express my thanks to, Professor Kishek for his encouragement and help, during the crucial phase of this project. The discussions and simulations with him made a big impact on the completion of this thesis. I am indebted to Dr.Santiago Bernal for teaching and helping me understand beam physics in general and beam matching in particular. His experimental works are of major influence to this project. I would also like to thank Dr.Sutter, for suggesting Collins scheme for injection.

There is a big experimental part to this project. To build a machine like UMER and to keep it running requires extreme care, hard work, and patience. I would like to thank Bryan Quinn and Dr.Walter for their support in the lab and more recently Brian and Cohen. It was a pleasure to work with them all. I am really grateful to Bryan Quinn and Mike Holloway for their help outside the lab. I would like to thank the graduate students Dr.Li, Diktys, Chris, Kai, Gang, Nathan, Todd and Chao. My thanks to Dr. Haber and Dr.Godlove for useful discussions. Thanks to Dr.Donald Feldman and Dr.Renee Feldman for their encouragement and help. Thanks to all the IREAP Staff.

I also thank US Department of Energy for their support to the UMER project.

I would like to thank my pastor Rev. Chandran Lite and his family, Roda Chandran Lite, Jacob Lite for their warmth, love and affection. Pastor Lite is a living example of the epitome of God's love. His enthusiasm for God's word and the church, his ability to use simple, vivid illustrations to make difficult doctrinal truths clear was remarkable. Pastor Lite and his family took great care of me and have considered me as part of their own family. I am greatly indebted to them for the rest of my life. Special thanks to Jacob for all those car rides and the songs that he shared with me.

Valentine annan has been of immense help to me. His panache, his highest regard for knowledge in life, his adaptability to any difficult circumstances in life makes him a rare genius and joy to be a friend with. He has been a very magnanimous and trustful friend. I can only aspire to be such an influence in someone else's life one day. I also thank his family, Sheba Valentine, Isaiah and Zenas for their affection. I am grateful to Edwin Thatha and Pattima for making sure that I stay focused and healthy during my studies. I would like to thank Mrs. Mala James and her family, Mano annan and Shanthi akka for their beloved support. Prince annan, Bhamini akka and Nathan deserve a special mention for their care and concern they showed. Prince annan's analytical thinking and his vast knowledge still amazes me! My thanks extend to the Bhaskaran family and Noble annan family for their enormous emotional support. Finally, I would like to thank the whole IFC congregation for their wonderful support throughout these years. IFC is a beautiful example of God's caring spirit.

I thank my roommate, Thangamani Veeramani for being a supportive and understanding friend. Thanks to my friend, Deepak Sridharan for his help during the

semesters, in and after school. Special thanks to Karthik, Eswaran and Ashwin for bringing Madras to Maryland with their lively presence and Tamil films. Thanks, Mahesh for all your timely help. I thank all other friends, who have helped me directly or indirectly on several different occasions.

I thank my parents and my brother for their brilliant lifelong examples of love, prayer, and their unwavering support and encouragement during these years. Above all I thank God, who has been my shepherd and light all these years and will be in my future endeavors.

# Table of Contents

Dedication.....	ii
Acknowledgements.....	iii
Table of Contents.....	vi
List of Tables.....	viii
List of Figures.....	ix
List of Figures.....	ix
Chapter 1: Introduction.....	1
1.1 Introduction.....	1
1.2 Background.....	1
1.2.1 Matched beam.....	1
1.2.2. Matching.....	2
1.2.3 Effects of mismatch.....	3
1.3 Motivation.....	4
1.4 Previous Work.....	4
1.5 Organization of the Thesis.....	5
Chapter 2: University of Maryland Electron Ring.....	7
2.1 Introduction.....	7
2.2 Motivation of UMER.....	7
2.3 Design of UMER.....	9
2.4 UMER Layout.....	10
2.4.1 Electron gun section.....	11
2.4.2 Matching/Injection section.....	12
2.4.3 Ring section.....	14
2.5 UMER Operation.....	15
2.5.1 Pulsed injection.....	16
2.5.2 UMER control interface.....	16
Chapter 3: Beam Matching Codes.....	18
3.1 Introduction.....	18
3.2 SPOT.....	19
3.2.1 Principles behind SPOT.....	19
3.2.2 Matching in SPOT.....	20
3.2.3 Features and limitations of SPOT.....	22
3.3 MENV.....	23
3.3.1 Principle behind MENV.....	23
3.3.2 Matching in MENV.....	23
3.3.3 Features and limitations of MENV.....	25
3.4 TRACE 3-D.....	26
3.4.1 Principle behind TRACE 3-D.....	26
3.4.2 Matching in TRACE 3D.....	27
3.4.3 Features and limitations of TRACE 3-D.....	28
3.5 Empirical Matching.....	29
3.6 Conclusion.....	31



Chapter 4: Matching of the Low Current Beam .....	32
4.1 Introduction.....	32
4.2 Matching of the Low Current Beam in UMER .....	32
4.2.1 Theory .....	33
4.2.2 Computer simulation.....	35
4.3 Conclusion .....	45
Chapter 5: Matching of the high current beam .....	46
5.1 Introduction.....	46
5.2 Matching of the high current beam in UMER .....	46
5.2.1 Computer Simulation.....	47
5.2.3 Experiment.....	51
5.3 Conclusion .....	54
Chapter 6: Conclusion.....	55
6.1 Suggestions for future work.....	55
Appendix – Collins Injection .....	57
Bibliography .....	60

## List of Tables

Table 1: UMER parameters .....	10
Table 2 Key parameters of Ring Quadrupole and Ring Dipole.....	15
Table 3 Calculated quadrupole settings for 0.55mA beam with 5.5 $\mu$ m .....	39
Table 4 Parameters for multi-turn for emittance dominated beam.....	44
Table 5 Calculated quadrupole settings for the 23.5mA beam with 20 $\mu$ m.....	50
Table 6 Parameters for multi-turn for a intense beam (23.5 mA).....	53
Table 7 Comparison between the Classic (Edge) Injection Vs Collins Injection.....	58

## List of Figures

Figure 1 A matched beam (23mA) showing smooth envelopes (X- blue, Y-red).....	2
Figure 2 UMER Operating Graph showing emittance and space charge dominated regime .....	9
Figure 3 UMER Schematic.....	11
Figure 4. Injection Section of the University of Maryland Electron Ring.....	12
Figure 5. Y-injection section.....	13
Figure 6 FODO Lattice - Magnets.....	14
Figure 7 Snapshot of SPOT- A matching program.....	21
Figure 8 Snapshot of MENV – A matching program in MATLAB.....	24
Figure 9 Snapshot of TRACE3D- A matching program .....	27
Figure 10 Empirical matching in WARP. Beam sizes before empirical matching (BLUE) and after (BLACK).....	30
Figure 11 Schematic of a periodic FODO Lattice in UMER.....	34
Figure 12 FODO Matching Calculation of pencil beam in MENV .....	36
Figure 13 Mechanical drawing of the injection line – Top View .....	37
Figure 14. Multi-turn/ recirculation matching for Y-magnets - pencil beam .....	38
Figure 15: Multi turn injection line matching for the pencil beam.....	38
Figure 16 Phosphor screen output of pencil beam from - IC1, IC2,RC1,RC2,RC3,RC5,RC6,RC7,RC9,RC12,RC14,RC16 .....	40
Figure 17 Experimental beam sizes Vs Expected beam sizes for the pencil beam ....	41
Figure 18 Multi turn BPM signal output from RC2- More than 100 turns.....	43
Figure 19: BPM Signal showing current loss after third turn and stabilizes thereafter .....	43
Figure 20 Beam current for the pencil beam Vs turn number. The thin black lines indicate the error bars in the measurement. ....	44
Figure 21 FODO Matching in TRACE3-D for high current (23.5 mA) beam.....	47
Figure 22 Top View of the Injection line along with the Y-section and recirculation section .....	48
Figure 23 Multi turn recirculation matching for 23mA beam .....	49
Figure 24 Injection line matching for 23mA beam.....	49
Figure 25 Empirical matching of 23mA beam in WARP (BLUE- Before: BLACK- After).....	51
Figure 26 Phosphor screen output of the 23mA beam.....	51
Figure 27 Measured beam sizes Vs expected beam size of the 23mA beam .....	52
Figure 28 Output of the BPM signal showing multi turn operation of the 23mA beam .....	53
Figure 29 Simulation of Collins injection scheme for the low current beam .....	58
Figure 30 Collins injection scheme for the high current beam showing large envelope excursion.....	59

# Chapter 1: Introduction

## 1.1 Introduction

The transport of intense beams with high beam quality is very important in advanced accelerator research. Intense beams envisioned for future free electron lasers, colliders, and heavy ion fusion systems have tight tolerance limits on emittance and beam size. The brightness requirements impose stringent limits on current loss over long distances. Accelerators are required to reduce the particle loss to the wall of the beam pipe in order to reduce the risk of radioactivation and increase safety. Future accelerators, then, will need beams of very small spot size that are well contained inside the transport systems and are transported with minimum current loss over long distances. These requirements necessitate good betatron matching of the beam. So, matching the beam is a crucial part in the design and operation of any future accelerator.

## 1.2 Background

### 1.2.1 Matched beam

A well matched beam will have a smooth envelope evolution inside the focusing lattice with minimal blowup. For a given emittance, the matched beam has

the smallest width as it propagates inside a focusing system. Moreover, full current transport of the beam is attained, in the case of a periodic focusing lattice, when a beam is perfectly matched. In a perfectly matched beam, propagating in a uniform focusing channel, the external focusing force is balanced by the internal defocusing space charge force and the thermal force due to the random velocities of the particles. A matched beam will also have minimum loss of particles and has been shown to prevent emittance growth and halo formation [1, 2]. An example of a matched beam is shown in Fig.1. A matched beam has envelopes that exhibit the minimum least squares deviation from the average beam size. In other words, the envelope of a matched beam has the same periodicity of the lattice.

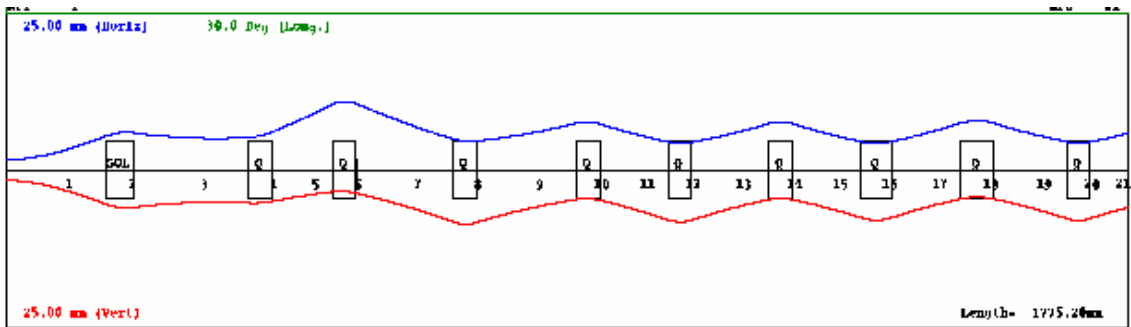


Figure 1 A matched beam (23mA) showing smooth envelopes (X- blue, Y-red)

### 1.2.2. Matching

Matching of a beam requires that the transport system is well designed, and the initial beam condition set up to match the transport system. So a matched beam transport depends on a combination of factors like beam emittance, beam current, good beam steering and good design. Precise knowledge of these parameters at the

beginning of the beamline will help to match a beam. In practice, perfect matching is often difficult to achieve as it depends on various factors.

The spacing between the focusing elements, the limiting current of the focusing element, the polarity, bends, and effective length of each element should all be taken into account in trying to match the beam [3]. In addition to the above, there are constraints like the initial conditions of the beam that are unknown and final conditions that are defined by the periodic focusing lattice. We must also consider proper matching conditions at locations, where lattices of different machines or beam transport systems meet. The injector section in the University of Maryland Electron Ring (UMER) is a good example.

Moreover, it is important to match the beam right at the beginning of the beam line with its initial distribution, because any attempt to compensate for initially mismatched beam at a later point along the beamline will lead to permanent emittance growth. Care must be taken to minimize defects like misalignment errors in an experimental setup, so that they do not disrupt the beam transport and hence mismatch the beam.

### 1.2.3 Effects of mismatch

Theoretical, simulation and experimental studies of emittance growth in a space charge dominated beam, suggests that initial mismatch as a key factor in causing emittance growth [4]. When a beam that has Courant-Snyder parameters different from the actual design parameters of the accelerator is injected into the accelerator transport lattice, it will have emittance increased due to nonlinearities and

filamentation [5]. When beams are injected with an initial mismatch, another mechanism called parametric resonance may cause formation of halo particles and beam emittance growth. In high-intensity accelerators, this will cause the pipe to become radioactive. An additional undesirable effect, when the beam injected into a focusing lattice is not well matched to the previous lattice is the development of envelope oscillations [3]. A matched beam has minimal envelope oscillations (Section 4.4.3 Ref [3]).

### 1.3 Motivation

One of the important problems in accelerator and beam transport design is to match the beam from one focusing system into a periodic focusing lattice. By varying the focusing strength of the lenses, the beam radius and slope is varied until desired matching condition is achieved.

The purpose of this thesis is to investigate the computational and experimental aspects of matching an emittance dominated beam (0.55mA) and a space-charge dominated beam (20.5mA) through the Y-injection and the ring lattice at the University of Maryland Electron Ring (UMER). Matching of the electron beam is studied with different schemes of injection and under different beam current.

### 1.4 Previous Work

Initial experimental work in this regard was done by S.Bernal et al [6].It was done on a 1-m long straight section containing the solenoid and the five printed

circuit quadrupoles. Further work was done in the computational aspects of developing new codes like SPOT, which was investigated by C.K.Allen [7] and then MENV by Hui [8]. Along the direction of experimental work, progress was made by Li Hui [9] through real-time empirical matching of a space charge dominated beam. Recently a review of the matching including general principles involved in betatron function matching along with experimental results and simulation study in UMER has been done by S.Bernal [10].All these previous studies were done on a D.C. injection system. This work is based on a new pulsed injection system. Currently, the injection is done through the fringe field of a pulsed magnet. Other recent developments in UMER like multi-turn operation and automated beam steering are discussed in the next chapter of this thesis.

## 1.5 Organization of the Thesis

This thesis work takes into account the new Y-injection section with new third generation quadrupoles and explores both an emittance dominated beam and a space charged dominated beam transport through the UMER geometry and over much longer transport distances.

In Chapter 2, the experimental setup, University of Maryland Electron Ring (UMER) is discussed. The motivation, ring layout and operating conditions of UMER are discussed. Recent results like multi-turn and automated beam steering are reported.

In Chapter 3, the different computer codes that are used for betatron matching is discussed. The different approaches used by each one of them for solving of the



matching problem are analyzed. Experimentally matching a beam requires simulations with more realistic codes like WARP and techniques like empirical matching. These are detailed in this chapter.

The computational and experimental results from matching an emittance dominated beam (0.6mA) are discussed in Chapter 4. UMER uses a 10-keV electron beam; therefore, the internal defocusing force from space-charge is an important factor. Matching a space-charge dominated beam (23mA) along with simulation and experimental results is discussed in Chapter 5.

Further in the appendix, techniques like Collins injection are discussed and preliminary results reported.

## Chapter 2: University of Maryland Electron Ring

### 2.1 Introduction

The ability to generate and transport intense, high quality beam is vital for advanced accelerator research. The problem is well modeled using low energy, high-intense electron beam and is being investigated at the University of Maryland Electron Ring (UMER). UMER is a compact yet complex machine. In the first part of this chapter, the physics and motivation behind UMER is discussed. In the second part of the chapter, the design, layout, and operation of UMER are covered. Recent progress like multi-turn operation is discussed at the end of the chapter.

### 2.2 Motivation of UMER

The basic motivation behind University of Maryland Electron Ring (UMER) [11-13] is to study space-charge phenomena of intense beams. The University of Maryland Electron Ring (UMER) is a scaled model to investigate the physics of intense beams. It uses a 10-keV electron beam along with other scaled beam parameters that model the larger machines but at a lower cost. All beams are born as space-charge dominated beams in the gun; hence the experimental and theoretical study of such beams will have important applications in future accelerators.

UMER is unique in a sense, that it is designed for beam experiments in ranging from low-current transport to highly space-charge dominated current

transport. The value of dimensionless intensity parameter  $\chi$ , gives a more clear idea about beam intensity. The intensity parameter  $\chi$  [14] is defined as the ratio of the external focusing force to the internal defocusing space-charge force. Mathematically,

it is given by  $\chi = \frac{K}{k_0^2 a^2}$ . The space-charge term is represented by  $\frac{K}{a}$ , where

$K = \frac{2I}{I_0 (\beta\gamma)^3}$ , is the generalized perveance,  $a$  is the beam radius,  $I$  is the beam current

,  $I_0 = 17$  kA for electrons,  $\beta$  is the ratio of the velocity of the electrons to the velocity

of light ( $v/c$ ) and  $\gamma$  is the Lorentz factor, given by  $\gamma = \frac{1}{(1-\beta^2)^{1/2}}$ . The external

focusing forces are represented by  $k_0$ , the zero-current betatron wavenumber. This  $k_0$

is related to 4 times rms emittance  $\epsilon$ , by the Kapchinsky-Vladimirsky (K-V)

transverse beam envelope equation of a matched beam, under smooth approximation

[3] as:  $k_0^2 = \frac{K}{a^2} + \frac{\epsilon^2}{a^4}$ .

The maximum value  $\chi$  can take is 1 and the minimum is 0. A zero current, emittance dominated beam corresponds to  $\chi = 0$ , while  $\chi = 1$  corresponds to a totally space charge dominated beam. So  $\chi = 0.5$  is the demarcation line. For a ranges  $0 < \chi < 0.5$ , the beam is emittance dominated but for  $0.5 < \chi < 1$ , the beam becomes space-charge dominated. The following figure shows the range of intensity parameter,  $\chi$ , swept by UMER. With  $\chi$  between 0.2-0.98, UMER gives access to, intense beam regime, which has hitherto been unexplored. Hence, the UMER facility will allow experimental investigations about the collective behavior of these beams like halo formation, space charge waves [15].

## Present UMER Operating Points

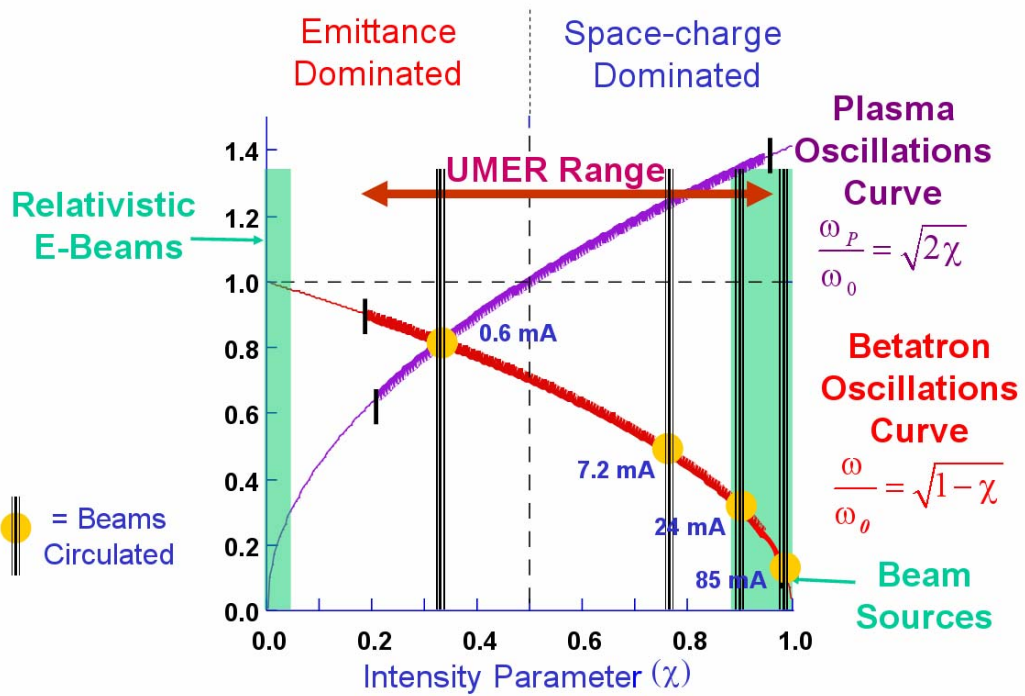


Figure 2 UMER Operating Graph showing emittance and space charge dominated regime

### 2.3 Design of UMER

UMER is designed to investigate low-energy beams; hence UMER will operate at a fixed energy of 10-keV. The pulses are 100ns long. As mentioned earlier, UMER allows a range of beam current from 0.55mA to 100mA. This is done by adjusting the collimating aperture near the exit of the electron gun box. Other important global design parameters are listed in the table below.

**Table 1: UMER parameters**

Beam Energy	10 (keV)
$\beta$	0.2
Current	0.55-100 (mA)
Emittance ( normalized,rms)	< 3.0 $\mu\text{m}$
Circumference	11.52 m
Pulse Length	20-100ns
Pulse repetition rate	60 Hz
Lap time	197 ns
Lattice Period	0.32 m
Zero-current Phase Advance	76°
Tune depression	> 0.16
No. of quads / No. of dipoles	72 / 36

## 2.4 UMER Layout

The schematic below shows the UMER layout. The layout can be divided into the following sections: electron gun section, matching/injection section and the ring section. The 10-keV electron beam is generated in the electron gun section. The electron beam is matched, transported in the matching/injection section before being injected into the ring lattice. The ring section does the focusing/bending and the beam is re-circulated for the next turn. At the time of this writing the extraction section is still in the design phase. In the following section, each of the UMER sections is discussed briefly.

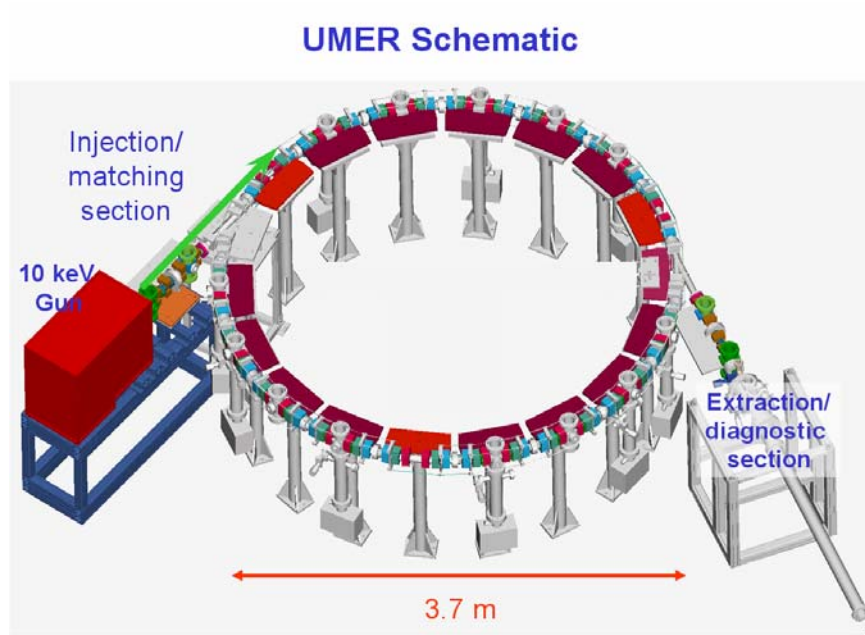


**Figure 3 UMER Schematic**

#### 2.4.1 Electron gun section

UMER employs a thermionic, gridded gun with a Pierce-type configuration. The anode is at ground potential, while the cathode and grid are at -10-keV. A complete description of UMER gun is outside the scope of this work. Further design features and simulations are discussed in [16-17]. The specific beam current needed for each experiment is obtained by changing the collimating mask on the aperture plate near the anode.

### 2.4.2 Matching/Injection section

The CAD drawing of the matching/injection section is shown in the figure below.

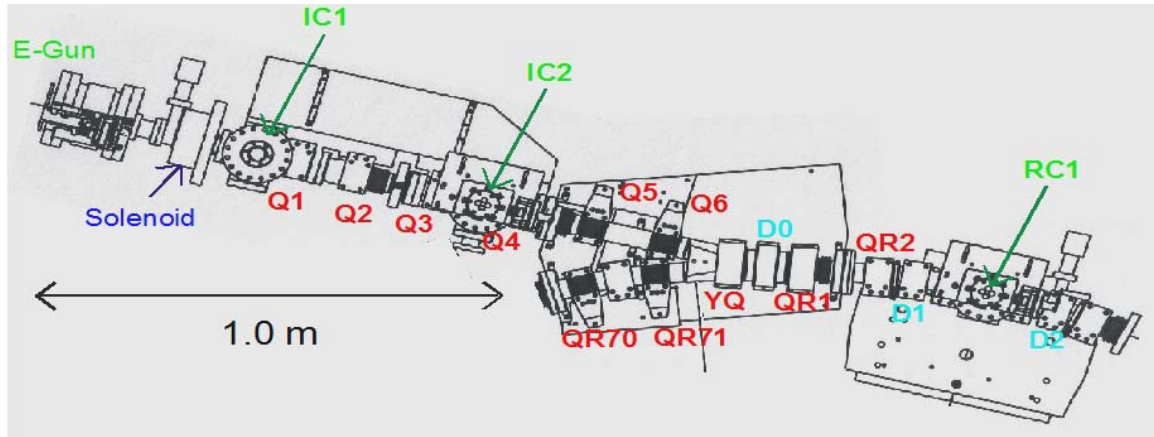


**Figure 4. Injection Section of the University of Maryland Electron Ring**

The injection section can be further divided into two sections: the straight section and the Y-section. The matching/injection section consists of six printed circuit quadrupoles (Q1-Q6) and a short solenoid in the beginning of the section. All these magnets are powered independently by DC power supply. These quadrupoles along with the solenoid perform the matching and the focusing of the electron beam from the electron gun. The steering of the electron beam in the focusing channel is done by six horizontal and six vertical short printed circuit dipoles (SD). There are also two diagnostic chambers on the section. The first one has a phosphor screen for imaging the beam while the second one has an additional fast beam position monitor (BPM) [18]. The BPM is used to determine the location of the beam centroid and hence used for beam steering purposes. The straight part of the injection section from Q1-Q4 is protected from effect of the earth's horizontal magnetic field by Helmholtz coils.

While the horizontal component of the earth's magnetic field is compensated by Helmholtz coils, the vertical component of the earth's magnetic field is used in bending the electron beam. The Y-section part of the injector is shown in the figure.

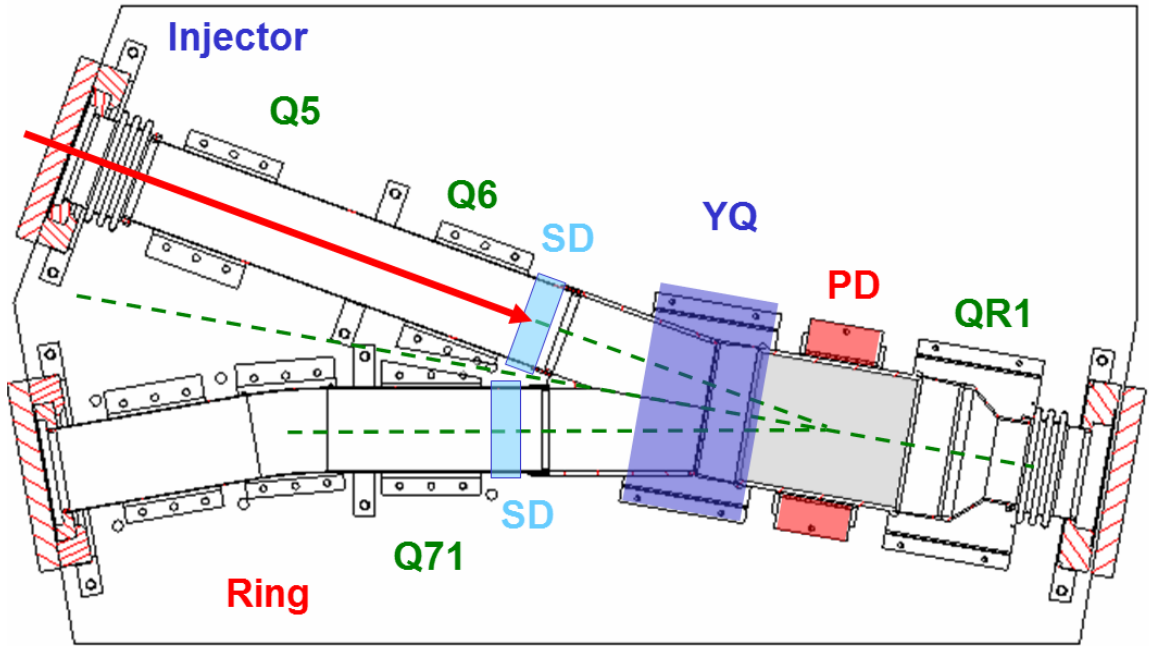


Figure 5. Y-injection section

The design of the Y-section is complex. The Y-section is composed of the flange from Q5 to the pulsed dipole (PD) and also the part of the ring-section from ring quadrupole Q70 to the pulsed dipole (PD). Both of these parts make a  $10^\circ$  angle with the ring section. The Y-section continues to extend from PD up to QR1. One of the key factors in the design of Y-section is the injection magnets, YQ and the QR1. Both of these magnets are Panofsky type and due to their big size draw higher current of 5.45 A. The YQ is shared by the two legs of the Y-section. It acts both as Q7 and Q72. The YQ is positioned off-centered to the beam trajectory and hence helps in bending the electron beam in addition to providing defocusing horizontally. Hence, both during injection and recirculation, it bends the beam into the ring and help in



steering. Further details on the electromechanical design of the Y-section are discussed in [19]. It should be noted that the Y-section is not shielded from the earth magnetic field. This adds to the complexity of steering and injecting the beam. The effect of earth's magnetic field on the Y-section and steering corrections involved are discussed in detail in [20].

### 2.4.3 Ring section

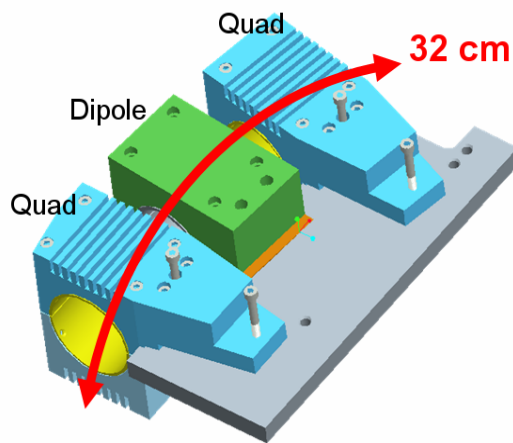


**Figure 6 FODO Lattice - Magnets**

The figure above shows a part of the ring section of UMER. It consists of two FODO section intercepted by a diagnostic chamber, which has a beam position monitor (BPM) and a phosphor screen. Each FODO is composed of a ten degree bend, two printed circuit quadrupoles and a printed circuit dipole. While one of the FODO quadrupoles acts as a focusing lens, the other quadrupole acts as a defocusing one. The printed circuit ring dipole does the bending of the electron beam in the ring. A vertical steering magnet is installed in each section. The whole ring consists of 36 FODO periods of length 32 cm. The ring circumference is 11.52 m. The zero-current phase advance per FODO period is  $76^\circ$ . The zero-current phase advance is an important design parameter and is used in matching calculation.

Just as in the straight section of the injection line, Helmholtz coils are used over the ring section to compensate for the horizontal component of the earth magnetic field. The vertical component of the earth's magnetic field provides one-third of the magnetic field required to bend the electron beam over one period. By providing this, it bends the beam around  $2^\circ$  for one FODO period. The main characteristics of the printed circuit (PC) ring quadrupole and printed circuit ring dipole is given in the table below. Further details of magnet design are discussed extensively in [21-22]. As an added note, second-generation quads will be phased out and third generation quadrupoles will replace the UMER ring.

**Table 2 Key parameters of Ring Quadrupole and Ring Dipole**

Element	Ring Quad (II generation)	Ring Quad (III generation)	Ring Dipole (Printed Circuit)
Peak on- axis gradient	4.14 G/cm-A	3.61 G/cm-A	5.22 G/A
Current	1.88 A	2.115 A	2.35 A
Effective Length	3.63 cm	3.72 cm	3.76 cm

## 2.5 UMER Operation

One of the goals of UMER is transport the low-current beam (0.55mA) to 100 turns and the high-current (100mA) for 10 turns. As mentioned before, the required electron beam is generated by changing the aperture near the exit of the gun assembly close to the anode. The injection of the beam is done by pulsed injection and the

beam steering is done by a computer controlled interface. These are described briefly in the following sections.

### 2.5.1 Pulsed injection

UMER operates on a 100ns long pulsed and at 10-keV, the beam circulation time around the ring is around 200ns. So, when the next pulse is injected by the pulsed dipole, the head of the beam is halfway around the ring. So, the pulsed dipole has less than 100ns to switch polarity to recirculate the returning beam. This requires careful and special electronic design to synchronize the timing sequences. A pulser has been designed and implemented in [23].

### 2.5.2 UMER control interface

UMER control is done mostly through a computer controlled interface. The current settings for the solenoid, injection/ring quadrupoles, dipoles and steering elements and their polarity are all controlled by a LabView [24] Interface under Linux [25]. This gives a much higher control and safer operation of UMER. Another important advantage is that, the BPM read outs are fed into the computer system through the oscilloscope. This makes the whole interface a feedback-loop based control system. So, by reading the BPM outputs, the interface can be programmed to change the current settings in the focusing elements. This helps in beam steering. Recently, the pulsed elements were also added to the control interface. Currently, the beam steering has been automated by a computer algorithm based on SVD technique.

An overview of progress details at the UMER project is discussed in [11] some of which are beam transport studies, matching of emittance and a space charge

dominated beam, etc. As of writing, multi-turn operation has been obtained in UMER. Further details on the recent progress along with multi-turn operation and beam steering (SVD) technique are discussed in [26]

The basic motivation and physics behind UMER was discussed earlier in this chapter. Later in the chapter, the design, the layout and operation of UMER were discussed. The chapter concluded by mentioning the recent multi-turn operation and automated beam steering. In the following chapter, the algorithms and the programs used to solve matching problem will be discussed.

## Chapter 3: Beam Matching Codes

### 3.1 Introduction

Matching an electron beam to the accelerator transport system is a complex analytical problem. A good estimate of the solution is best got using a computer simulation. In this chapter the matching codes used to match the electron beam in the University of Maryland Electron Ring (UMER) will be discussed. All codes solve the matching problem by integrating the envelope equation but each code takes a different approach to do the same. All the codes solve the beam envelope equation:

$$\begin{aligned} X'' + \kappa_x(z)X - \frac{2K}{X+Y} - \frac{\varepsilon_x^2}{X^3} &= 0 \\ Y'' + \kappa_y(z)Y - \frac{2K}{X+Y} - \frac{\varepsilon_y^2}{Y^3} &= 0 \end{aligned} \tag{3.1.1}$$

where the prime indicated differentiation with respect to  $z$ ,  $K$  is the generalized beam perveance, and  $\varepsilon_x$  and  $\varepsilon_y$  are the effective emittance of the beam in the  $x$  and  $y$  planes. The kappa  $\kappa_x(z)$  and  $\kappa_y(z)$  represent the focusing/defocusing strength of the transport system in the  $x$  and  $y$  planes.

In the above mentioned beam envelope equation is a second order differential equation in four variables and needs four initial conditions. In a transport system, the

matching section is used to match a beam from input section to a periodic envelope section. Thus, we must satisfy the following four boundary conditions:

$$\begin{aligned}
 X(z_i) &= X_i, X(z_f) = X_f \\
 X'(z_i) &= X'_i, X'(z_f) = X'_f \\
 Y(z_i) &= Y_i, Y(z_f) = Y_f \\
 Y'(z_i) &= Y'_i, Y'(z_f) = Y'_f
 \end{aligned}
 \tag{3.1.2}$$

where  $(X_i, X'_i), (Y_i, Y'_i)$  is the initial beam position and slope at the entrance of the transport system  $Z = Z_i$  in the x and y plane respectively. In matching section, where the beam has to be matched onto a periodic system, the final conditions of the beam position and slope at the exit of the matching systems at  $Z = Z_f$  is given by  $(X_f, X'_f), (Y_f, Y'_f)$  for x and y planes respectively.

The codes used in UMER are SPOT [27, 28], MENV [8] and Trace3D [29, 30]. These codes along with WARP [30, 31] for empirical matching will be discussed in this chapter.

## 3.2 SPOT

### 3.2.1 Principles behind SPOT

SPOT is written based on optimal control theory to solve the beam transport and matching problem. The idea is to match the beam envelope to a design trajectory called “reference trajectory” in SPOT.

The heart of the SPOT program is to calculate and minimize the distance between the reference trajectory  $(\bar{X}(z), \bar{Y}(z))$ , chosen by the designer and the

solution trajectory  $(X(z), Y(z))$  that satisfies the envelope equation (3.1.1) and the boundary conditions (3.1.2). This can be represented as cost function say  $J$ . The target parameters, representing the boundary conditions, can be included in the  $J$  function as say  $\Phi$ , the target state function. So SPOT minimizes the sum of  $J$  and  $\Phi$   $J[X(z), Y(z)] + \Phi[X(z_f), Y(z_f)]$ , where

$$J[X(z), Y(z)] \equiv \frac{1}{2} \int_{z_i}^{z_f} [(X(z) - \bar{X}(z))^2 + (Y(z) - \bar{Y}(z))^2] dz \quad \text{and}$$

$$\Phi[X(z_f), Y(z_f)] = [W_1 X(z_f) - W_2 X_f]^2 + [W_3 Y(z_f) - W_4 Y_f]^2$$

$(W_1, W_2, W_3, W_4)$  are called the terminal weights and makes the optimization routine adaptable to tuning. For example, by increasing the values of the terminal weights, the optimizer can be made to converge to the terminal state faster as the optimization varies based on the terminal weights. Further details about SPOT can be found in [27, 28].

### 3.2.2 Matching in SPOT

SPOT is a computer aided design program that runs under Microsoft Windows in a PC. A snapshot of the program is shown below:

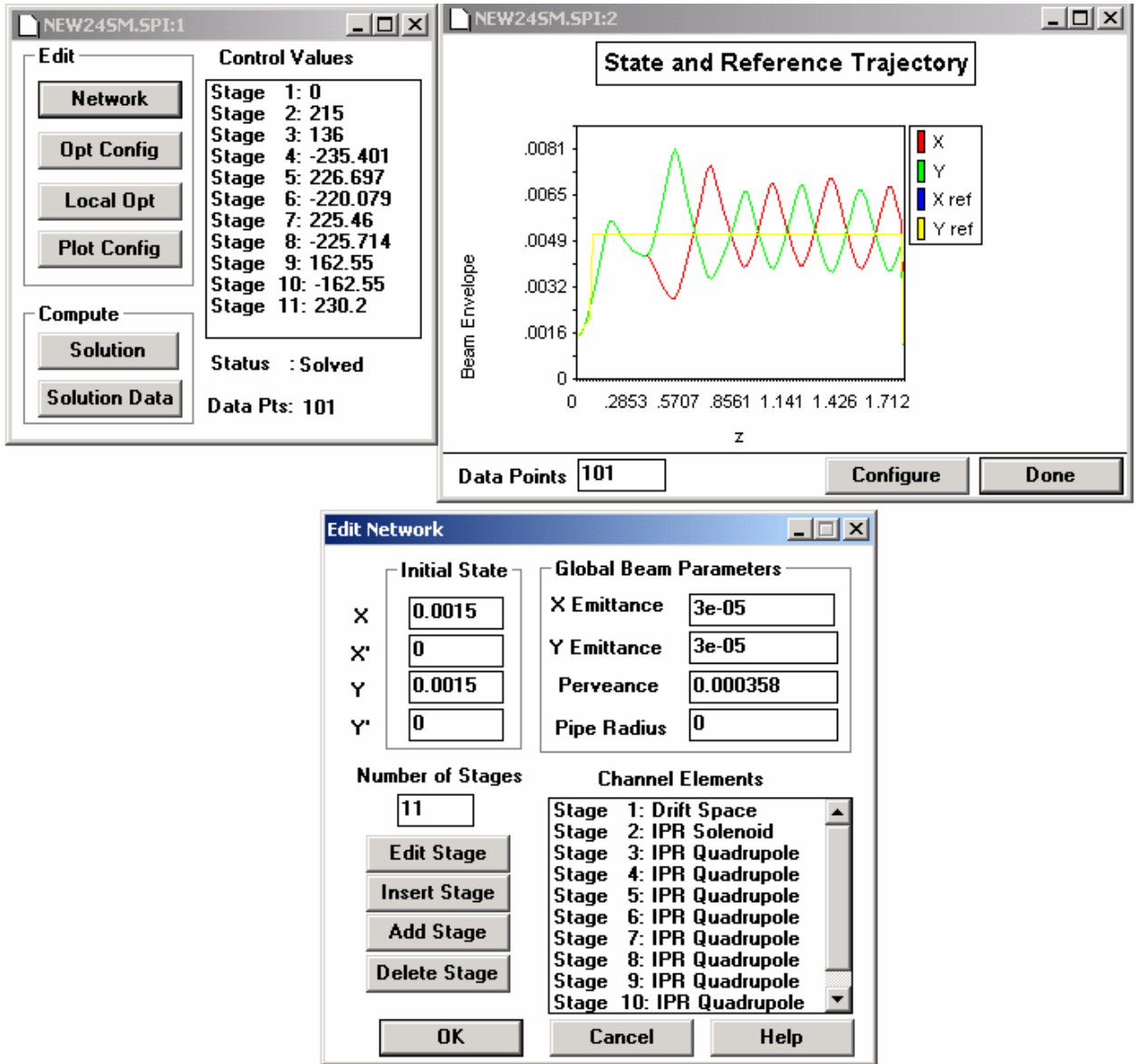


Figure 7 Snapshot of SPOT- A matching program

SPOT is an environment where the beam matching solution can be optimized in an interactive manner with the operator. This helps in getting a set of matching solution fast. Each beamline element like quadrupole, drift and dipole is added in stages. Once the transport system is setup, the beam parameters like emittance,



perveance and initial state are specified. The final state is calculated from matching the FODO lattice for a specific phase advance, ( $\sigma_0 = 76^0$ ) in UMER. The calculations to find the X, X', Y, Y' for a periodic FODO lattice can be done by SPOT. In fact, the smooth profile modeling of the quadrupoles in SPOT makes it the best choice for calculating the final state of the beam in the matching section, which matches the beam into a periodic lattice.

### 3.2.3 Features and limitations of SPOT

The attractive features of SPOT are its speed and smooth profile modeling of magnets. The speed comes from the numerical integration techniques employed while calculating the cost function J by first calculating the gradient. Once the gradient is calculated, non-linear programming is used to search for minimizing the set of kappas  $\kappa_x(z)$ ,  $\kappa_y(z)$ . Smooth profile modeling of the quadrupole magnets allows more accurate calculations for the focusing /defocusing strength of the magnets in the matching section as well as the periodic lattice.

The major disadvantage of SPOT is that the search technique employed picks out only local minimum that is nearest to the starting guess. The designer must provide the starting guess to SPOT. So the solution that SPOT provides might not be the best solution for the beam transport system under analysis. Another operating limitation of SPOT is the maximum number of beamline elements it can handle. Finally, existing version of SPOT cannot handle bends. When the number of beamline elements gets large, SPOT finds it difficult to converge or it takes a long time to converge. So SPOT is better suited for beam lines with fewer focusing elements.

### 3.3 MENV

#### 3.3.1 Principle behind MENV

MENV is a beam envelope solver and an optimizer written in MATLAB [33] by Hui Li [8]. MENV also solves the two dimensional envelope equations (3.2.1). MENV can be used to solve for periodic FODO lattice or for a matching section.

The main idea behind MENV is that it treats the matching problem as a nonlinear least squares and non-linear data fitting problem. Starting with an initial guess for the values of the focusing/defocusing quads, initial  $(X_0, X'_0, Y_0, Y'_0)$ , and final beam  $(X_f, X'_f, Y_f, Y'_f)$  conditions, MENV integrates the beam envelope equation from the initial values at  $Z = Z_i$  to get the final beam conditions at  $Z = Z_f$  for a set of kappa's  $\kappa_x(z)$ ,  $\kappa_y(z)$ . The beam's final conditions at  $Z = Z_f$  is say  $(X, X', Y, Y')$  MENV now calculates and minimizes the function

$$\min F(x) = \left\| \left[ (X - X_f)^2 + (Y - Y_f)^2 + (X' - X'_f)^2 + (Y' - Y'_f)^2 \right] \right\|^2$$

for different values of  $\kappa_x(z)$ ,  $\kappa_y(z)$ . The details of the algorithm can be found in [34,35]. There are also terminal weights in MENV, but they are typically left untouched.

#### 3.3.2 Matching in MENV



**Figure 8 Snapshot of MENV – A matching program in MATLAB**

MENV is run under MATLAB environment and hence can either be run in Microsoft Windows or Linux. Each beamline element such as a quadrupole, drift and dipole is inserted in steps to define the lattice. While entering the elements, other necessary inputs like effective length, location and kappas are also entered. Once the transport system is setup, the beam parameters like emittance, perveance and initial state are specified under solving parameter dialog box. The final state is calculated from matching the FODO lattice for a specific phase advance, ( $\sigma_0 = 76^0$ ) in UMER. This step of finding the X, X', Y, Y' for a periodic FODO lattice can done by MENV. But

we typically do this step in SPOT, because MENV uses hard-edge model for magnets which is less accurate than the smooth profile used by SPOT. Depending on the type of problem that is under study, either the matcher section or periodic matcher is executed. MENV is very fast and can converge even under tight limits on quadrupoles pretty quickly compared to SPOT.

### 3.3.3 Features and limitations of MENV

The key feature of MENV is the superb convergence under hard limits on the quadrupole strength. This is due to the fact it treats the problem as a nonlinear least square data fitting problem. It uses an optimization algorithm, which approximates the solution of a large linear system using a specialized method [29,30]. Another feature of MENV is its capability to fix certain quadrupole strength during matching calculations and to vary only other quadrupoles. The execution speed of MENV can be increased or decreased by changing the step size of the integration in the matcher parameters.

One of the shortcomings of MENV is that it models both the solenoid and quadrupole as hard-edge profile. This makes MENV less accurate compared to SPOT. So, fringe field effects are not at all taken into account. It uses a second-order leap frog algorithm for integrating the beam envelope equation and hence this makes MENV a bit slow compared to SPOT. This is a compromise paid for the convergence of MENV. As mentioned earlier, MENV is able to come up with best solution every under tight limits like for example a pencil beam.

## 3.4 TRACE 3-D

### 3.4.1 Principle behind TRACE 3-D

TRACE 3-D [30] calculates the envelopes of a bunched beam through a beam transport system, that is defined by the designer. TRACE 3-D takes into account linear space-charge forces.

The fundamental assumption in TRACE 3-D is that all forces affecting a beam can be linearized. The beam itself is represented by a 6X6 matrix called the  $\sigma$ - matrix. The  $\sigma$ - matrix defines a hyper ellipsoid in six-dimensional phase space. But for most calculation purposes, the useful projections planes are the transverse and the longitudinal planes, which are ellipses in each plane. These ellipses are described by Courant-Snyder parameters or Twiss parameters and the emittances in their respective planes.

TRACE 3-D tracks the beam through the beam line by a sequence of matrix transformation for each of the beam line elements. Hence, TRACE 3-D is a matrix based code and hence can provide immediate graphics display of envelopes and phase-space ellipses. These make TRACE 3-D a very useful design program.

At the core of TRACE 3-D, for each beamline element, a 6X6 matrix  $R$ , called transfer matrix is constructed. Let the  $\sigma$ - matrix at location  $s_1$  in the transport system by  $\sigma (s_1)$ . If the transfer matrix between two locations  $s_1$  and  $s_2$  is known, the beam matrix at  $s_2$ , can be calculated by a series of transfer matrix multiplication

$$\sigma (s_2) = R \sigma (s_1) R^T$$

TRACE 3-D allows lot of different elements to be in the beamline like RF gap, wiggler, doublet, and triplet. Further information about TRACE 3-D can be found in [30].

### 3.4.2 Matching in TRACE 3D

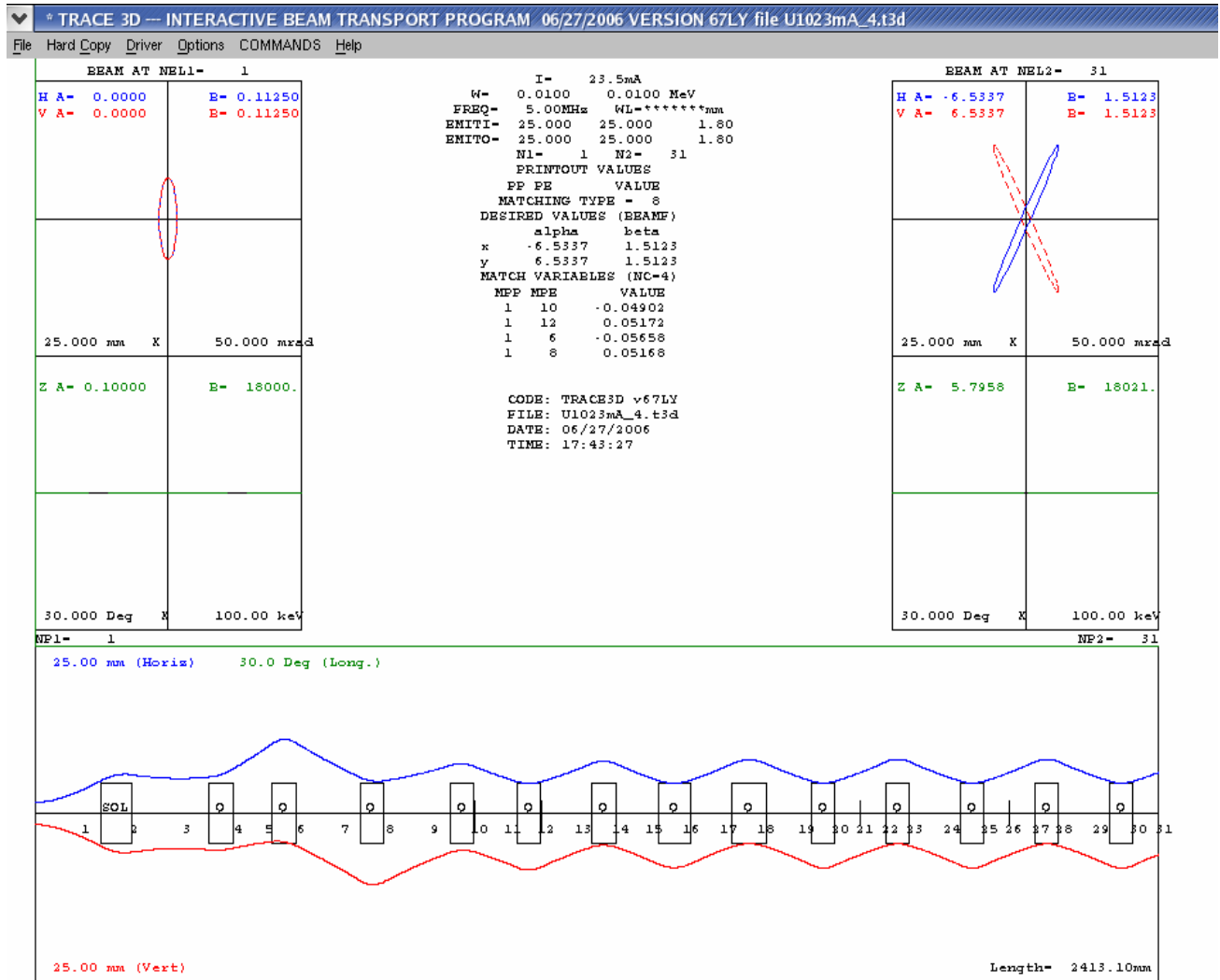


Figure 9 Snapshot of TRACE3D- A matching program

TRACE 3-D runs under Linux and there is a GUI interface PBOLab [29] written for Windows also. The description of the beam transport system is fed to TRACE 3-D through an input file, wherein the beam parameters and the beamline elements are defined. Each beamline element has a representative matrix. Hence, the matrix parameters have to be specified for all the beamline elements. For example, for quadrupoles, the location, the strength, and the effective length have to be given. One of the features of TRACE 3-D is the input of Courant-Snyder parameters for the description of the beam. Care should be exercised in converting from the Twiss parameters to the real beam phase-space parameters because emittance is described in a different manner in TRACE 3-D [30]. Once the input deck is completed, the TRACE 3-D program is loaded. TRACE 3-D then waits for single character input, which can be found in the documentation.

TRACE 3-D will draw a simple graphic display of the input, output phase-space ellipses and the beam envelopes over the transport elements. Depending on the matching parameter given in the input deck, the TRACE 3-D is iteratively executed to match the beam envelope to the transport lattice. This makes TRACE 3-D an interactive environment for the designer.

### 3.4.3 Features and limitations of TRACE 3-D

One of the advantages of TRACE 3-D is that it is a very flexible code and can handle bends, smooth-profile magnets (represented as Permanent Magnet Quadrupoles (PMQ)), RF gaps, etc... It is a standard code used by the accelerator community for quick beam transport calculations. Moreover, since the input is a well

structured deck, input decks can be generated by using scripting programs written in Python.

One of the limitations of TRACE3-D, though, is its simple graphic display. Another limitation of TRACE 3-D is its slow convergence of matching solution, if the number of beam elements becomes larger.

### 3.5 Empirical Matching

The matching calculations done by the matching codes do not take into account uncertainties in measuring beam current, initial beam conditions, and beam emittance. Another feature the codes lack is, that the earth's magnetic field is neglected, whereas in real beam experiments, these cannot be neglected. So, real time adjustment of the magnet strength, according to the various parameters becomes imperative [9]. This is the idea behind empirical matching.

Empirical matching is represented in a matrix form:

$$\begin{pmatrix} X_1 \\ Y_1 \\ X_2 \\ Y_2 \\ \dots \\ X_n \\ Y_n \end{pmatrix} = \begin{bmatrix} R_{x11} & R_{x12} & R_{x13} & R_{x14} & 1 & 0 \\ R_{y11} & R_{y12} & R_{y13} & R_{y14} & 0 & 1 \\ R_{x21} & R_{x22} & R_{x23} & R_{x24} & 1 & 0 \\ R_{y21} & R_{y22} & R_{y23} & R_{y24} & 0 & 1 \\ \dots & \dots & \dots & \dots & \dots & \dots \\ R_{xm1} & R_{xm2} & R_{xm3} & R_{xm4} & 1 & 0 \\ R_{ym1} & R_{ym2} & R_{ym3} & R_{ym4} & 0 & 1 \end{bmatrix} \begin{pmatrix} \Delta I_1 \\ \Delta I_2 \\ \Delta I_3 \\ \Delta I_4 \\ X_m \\ Y_m \end{pmatrix} \quad (3.5.1)$$

where  $X_i, Y_i$  are the  $2 \times$  rms beam sizes in the two transverse directions at the  $i$ -th diagnostic chamber when  $I_j$  is the current in the quadrupole  $j$ .  $X_m, Y_m$  are the matched  $2 \times$  rms beam sizes at the chamber location.  $\Delta I_j$  are the desired current



changes to minimize the mismatches at the quad. This is the amount by which the quadrupole has to be changed and this is the unknown quantity.  $R_{xij} = \partial X_i / \partial I_j, R_{yij} = \partial Y_i / \partial I_j$  are the changes in  $X_i, Y_i$  with respect to the current change in the quadrupole  $j$ . Let us denote the right-hand side of the equation 3.5.1 as  $E$ . Let us denote the unknown quantity by  $U$ . Then the solution for  $U$  in a least square sense is:  $U = (R^T R)^{-1} R^T E$ . Once the  $U$  matrix is found the optimal current in quadrupole  $j$  is  $I_j - \Delta I_j$ .

Empirical matching though typically is performed online in the lab can also be done using PIC codes like WARP [31, 32]. WARP can be used to do empirical matching because it has the capabilities to simulate complex geometry of the beam line, more real world profile for the quadrupole magnets and other nonlinearities.

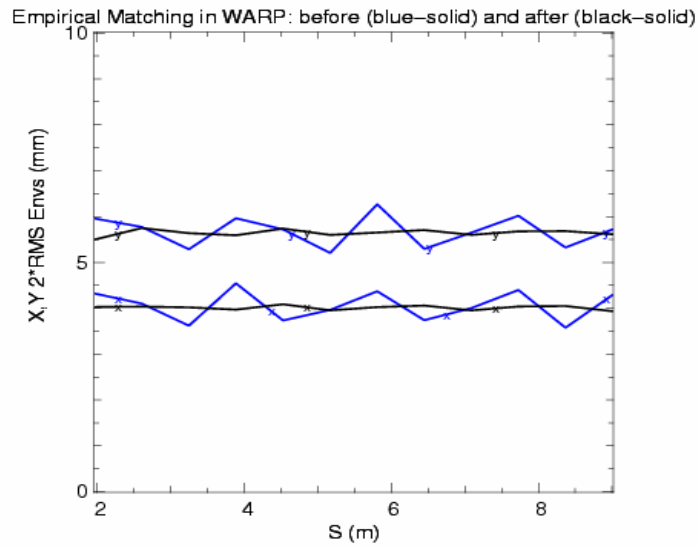


**Figure 10 Empirical matching in WARP. Beam sizes before empirical matching (BLUE) and after (BLACK)**

### 3.6 Conclusion

In this chapter various computer codes used for beam matching in UMER has been discussed. Each code has some unique feature and few limitations. So while doing matching calculations, the code to be used is chose based on the problem we are trying to solve. If we are solving for periodic lattice, we chose SPOT. If the problem in hand is to match a pencil beam, we use MENV. So the different approaches taken by each code complement each other in solving the problem of beam matching.

## Chapter 4: Matching of the Low Current Beam

### 4.1 Introduction

UMER is built to study space-charge dominated beams. However, UMER is a storage ring and hence understanding the low current beam will help in tuning the machine and in understanding beam steering and multi-turn operation. In order to have full current transport of the low current beam, the low current beam has to be matched to the transport system. In this chapter, the matching of the low current beam in UMER is discussed along with the theory, calculation and experiments. Through proper matching and steering, multi-turn operation of the low current beam has been achieved [1].

### 4.2 Matching of the Low Current Beam in UMER

The low current beam, or pencil beam, measures about 0.55mA -0.6mA. The low current beam is obtained by changing the aperture radius to 0.25 mm. The beam emittance of the pencil beam is 5.5 $\mu$ m. This refers to the 4 $\times$  rms beam emittance (unnormalized). The beam radius of the matched pencil beam is around 1.4 mm.

Consider the case of a circular beam traveling through a uniform focusing channel. We know from the K-V envelope equation that

$$R'' + k_0^2 R - \frac{K}{R} - \frac{\varepsilon^2}{R^3} = 0$$

where R represents the beam radius, K represents the beam perveance and  $k_0$  represents the external focusing force, and  $\varepsilon$  the emittance of the beam. The special

case of the solution to the envelope equation, when the radius of the beam is constant,  $R(z)=a$ ,  $R'(z)=0$  and  $R''(z)=0$ , the equation becomes:

$$k_0^2 a - \frac{K}{a} - \frac{\varepsilon^2}{a^3} = 0$$

When the above conditions are satisfied, the beam is said to be matched (See section 4.3.2 in Ref [3]). When the external focusing force ( $k_0$  is constant), the second term represents the defocusing space charge force and the third term is due to the emittance or thermal pressure. So, depending on which term dominates we can speak of two regimes, space-charge dominated regime and emittance-dominated regime. In the case of a low current beam,  $K= 8.0882e-6$ ,  $\varepsilon= 5.5\mu\text{m}$  and  $a= 1.5\text{mm}$  and hence  $\varepsilon^2 > Ka^2$ , and hence it is a beam in the emittance dominated regime. The tune of the low current beam is 6.36, making the tune shift from the zero-current tune to be 0.83, and hence  $\chi= 0.29$ .

#### 4.2.1 Theory

The fundamental unit, which constitutes the UMER ring, is the FODO lattice, which is depicted in the figure below. It is defined by a quadrupole of length  $l$  that is focusing in  $x$  and defocusing in  $y$ , and another quadrupole of equal length but defocusing in  $x$  and focusing in  $y$ . These two quadrupoles are separated by two drift sections, each of length  $L$ . The beam has to be matched into the FODO lattice. But, in order to be matched to the FODO lattice, we need the conditions (target state) that will be provided by the matching section between the gun and the ring. For a given

zero current phase advance of  $\sigma = 76^\circ$ , the effective length of the focusing magnets, and drift space between them, following Courant-Snyder theory we get:

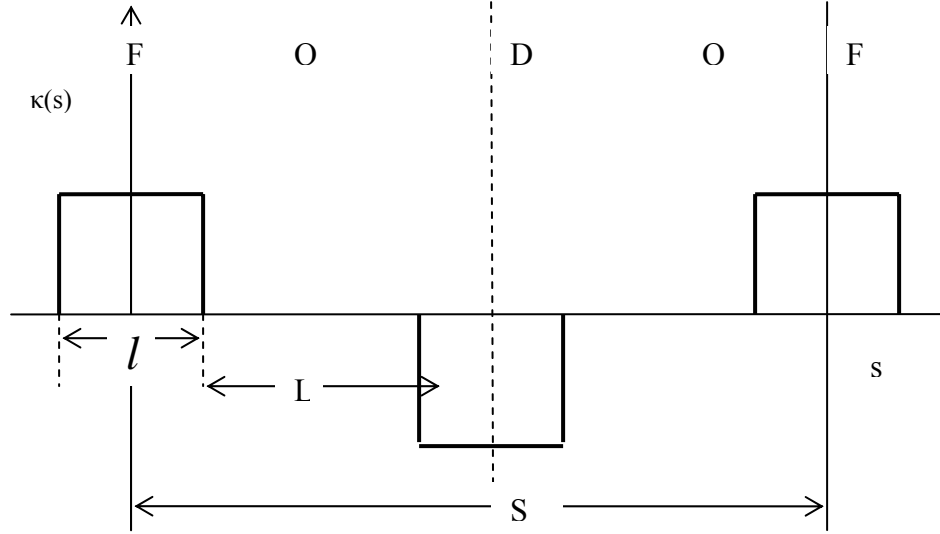


**Figure 11 Schematic of a periodic FODO Lattice in UMER**

$$\begin{aligned} \cos \sigma &= \cos \theta \cosh \theta + \frac{L}{l} \theta (\cos \theta \sinh \theta - \sin \theta \cosh \theta) \\ &\quad - \frac{1}{2} \left( \frac{L}{l} \right)^2 \theta^2 \sin \theta \cosh \theta \end{aligned} \quad 4.2.1.1$$

$$\theta = \kappa^{\frac{1}{2}} l$$

,  $\kappa$  is found out by solving the above transcendental equation using a computer. Then the current needed to the quadrupoles is found using the relation:

$$\kappa = \frac{q \left( \frac{B_0}{a} \right)}{\gamma m \beta c}, \text{ where } q \text{ is the charge of an electron, } \frac{B_0}{a} \text{ is the gradient in (G/cm-A), } \gamma \text{ is}$$

the Lorentz factor, and  $\beta$  is the velocity of the electron compared to the speed of light,

$c$ . Once kappa  $\kappa$  is found, the value of  $X, X', Y, Y'$  for which the beam envelope is periodic with the periodicity of the lattice is calculated. These values depend on the

beam current and the emittance. The matching section should match to these value of  $X, X', Y, Y'$  as the target state.

In the matching section in the injector, the magnet strength of the six quadrupole magnets and the solenoid is varied until the desired target state is obtained at the FODO inside the ring. Depending on the scheme of injection, the YQ and QR1 are kept at constant value, by treating them as part of FODO or switched off (Collins injection).

#### 4.2.2 Computer simulation

##### 4.2.2.1 Matching FODO lattice

The matching calculation starts from the periodic FODO lattice. Basically, a computer code solves the K-V envelope equation for different initial conditions until

$$X(z+S)=X(z), Y(z+S)=Y(z), \text{ and } X'(z+S)=X'(z), Y'(z+S)=Y'(z),$$

where  $S$  is the lattice period of 32 cm. The following figure illustrates the same using MENV.

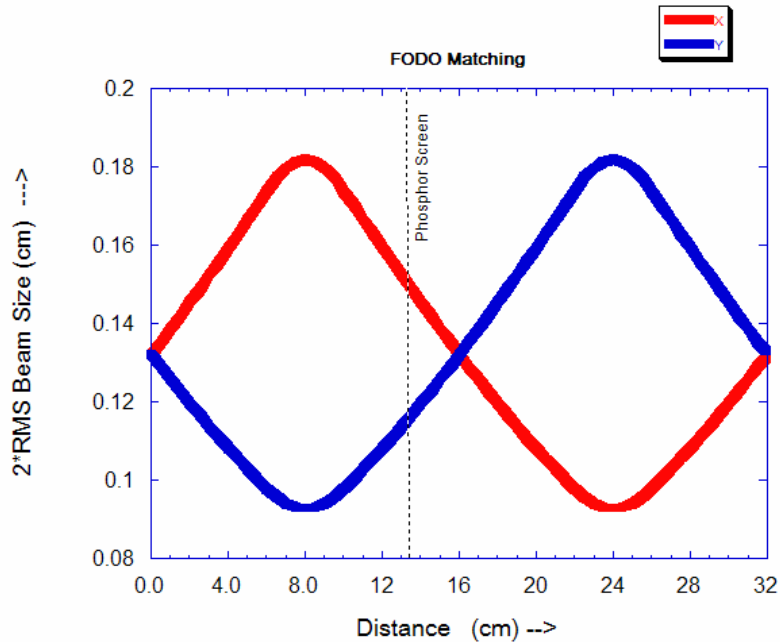


**Figure 12 FODO Matching Calculation of pencil beam in MENV**

From the above simulation, we can also calculate the expected beam size at the phosphor screen. For the pencil beam  $X = 1.5$  mm, and  $Y = 1.2$  mm. It is seen that the beam size in x-plane is larger than in the y-plane and hence we should expect to see an elliptical beam in every phosphor screen around the ring. The above calculation in MENV, as described in the earlier chapter, uses a hard-edge model for its magnet profile. SPOT calculations are used to get more accurate result, as SPOT models the magnet using a smooth profile.

#### 4.2.2.2 Matching section

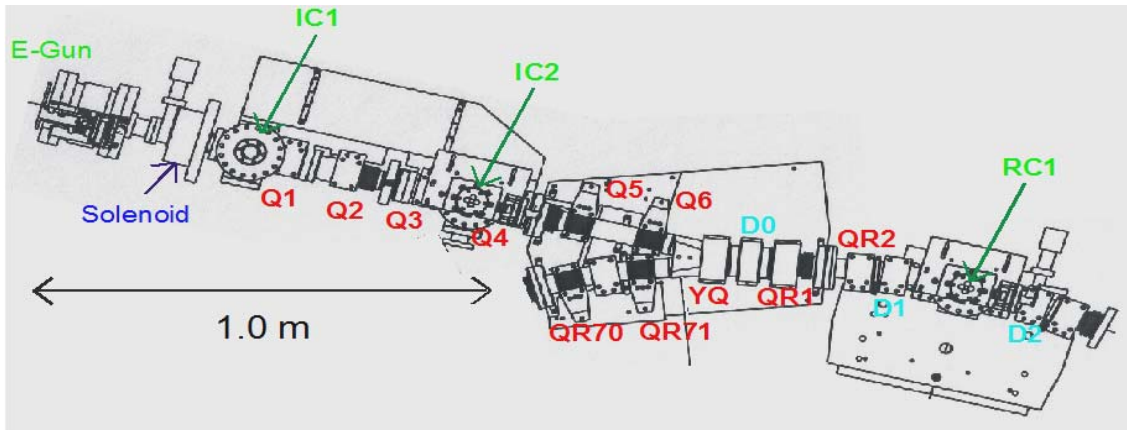


**Figure 13 Mechanical drawing of the injection line – Top View**

The above figure depicts the Y-injection section along with the matching section and the ring-section. The matching section consists of solenoid, Q1- Q6 and measures around 1.4 m. YQ, QR1 are big Panofsky magnets and are referred as Y-magnets. QR70, QR71 along with the Y-magnets forms the recirculation part of the ring and Q1, Q2 along with the Y-magnets constitutes the injection part of the ring. Calculating the magnets strength in the matching section is done in stages: First, the ring is solved for recirculation and then solved for injection. This is a crucial design step for multi-turn operation of the machine.

Once the single FODO lattice is run, the necessary target state to be matched becomes available. First, the recirculation section constituting QR71, YQ, QR1, QR2 is matched to get the current settings to match onto the FODO lattice. After this step, the current in YQ, QR1 and QR2 is fixed to the calculated value in the subsequent steps.



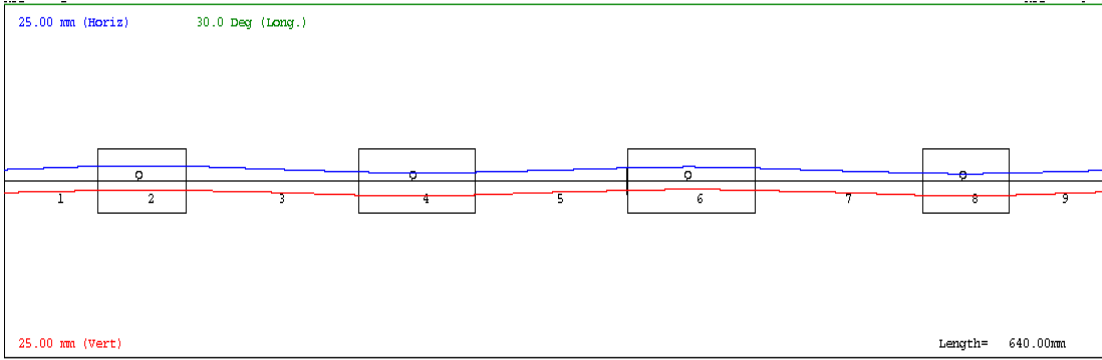


**Figure 14. Multi-turn/ recirculation matching for Y-magnets - pencil beam**

Now, once the values necessary for YQ, QR1 and QR2 is found out, the injector section from solenoid to Q6 is run through the matching program to yield the necessary target state at the FODO Lattice. Note during this step, YQ, QR1 and QR2 is fixed. We found that turning off Q1 and fixing the solenoid to around 90 Gauss yielded the best solution for the pencil beam. The matching program is run to obtain the optimal values of current settings on Q2-Q6. Good choices of initial values can lead to quick convergence.

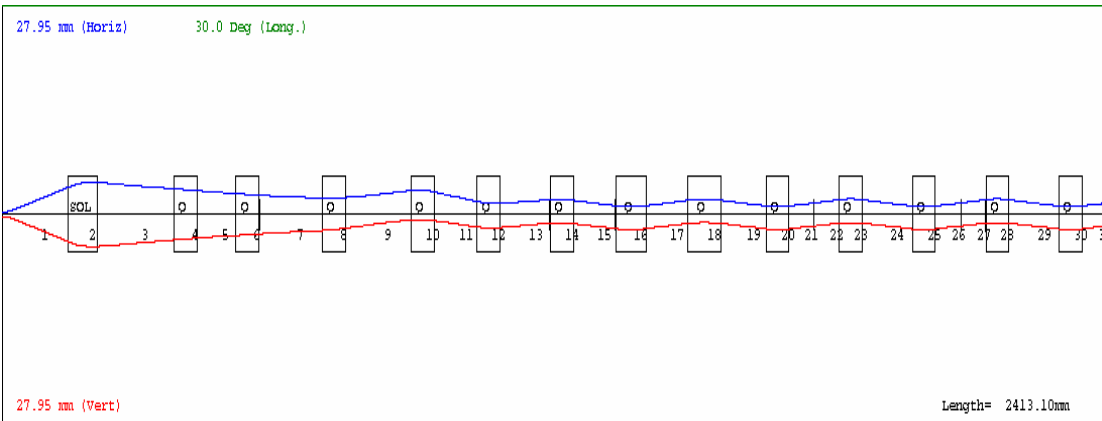


**Figure 15: Multi turn injection line matching for the pencil beam**

The values of the injector section settings and the FODO lattice settings for the transport of 0.6mA beam current and 5.5 $\mu$ m emittance are tabulated in the table below:

**Table 3 Calculated quadrupole settings for 0.55mA beam with 5.5 $\mu$ m**

<b>Magnet</b>	<b>Position (cm)</b>	<b>Current(A)</b>
Solenoid	17.5	4.92
Q1	40.0	0
Q2	53.5	0
Q3	72.41	0.91
Q4	91.79	1.71
Q5	106.15	2.43
Q6	122.14	1.79
YQ	137.31	5.43
QR1	153.31	5.52
QR2	169.31	1.93
QR3-QR69	185.31[+16 for every quad]	1.88
QR70	1257.31	2.11
QR71	1273.31	2.15

#### 4.2.1 Experiment

##### 4.2.1.1 Single-turn experiment

The low current beam is obtained by changing the aperture radius to 0.25 mm. All the quadrupoles, dipoles and the pulsed elements are set to the required current values using the LabView interface. The beam steering and alignment through the matching section was done through beam position monitors (BPM) placed in the diagnostic chamber. It should be noted that aligning the beam in the injector was done by reading the output of BPM RC1, which differs from the previous method of steering implemented by Hui Li using the phosphor screen [Ref]. Phosphor screen photos of a 10 keV, 0.55mA, 100ns beam is shown below:

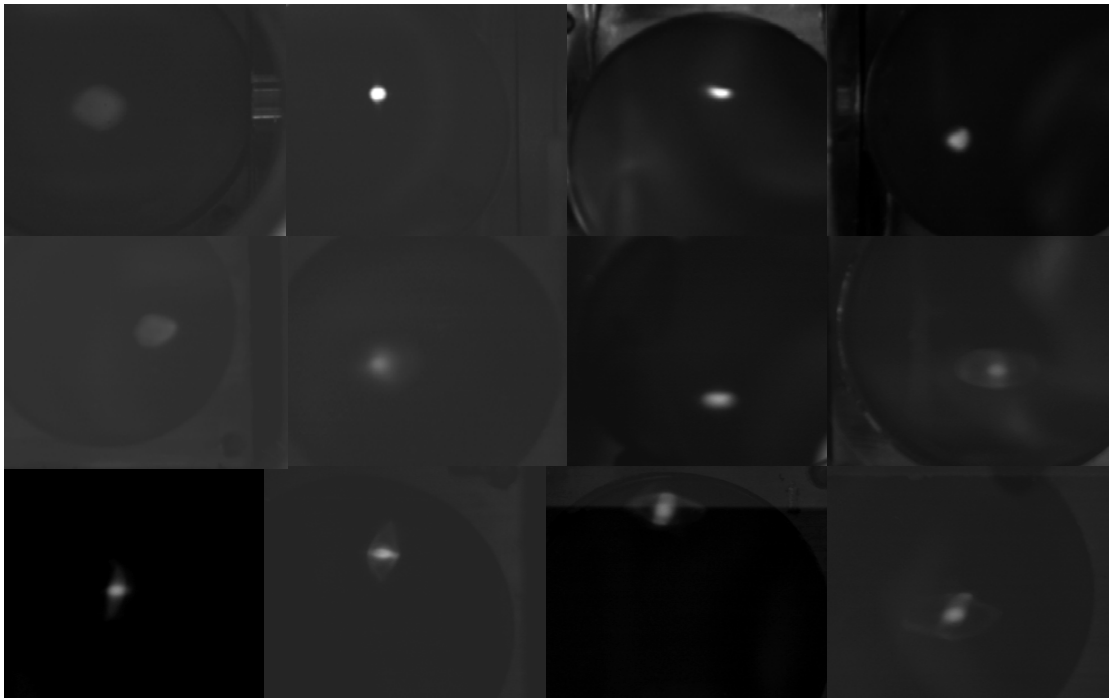


**Figure 16 Phosphor screen output of pencil beam from - IC1, IC2,RC1,RC2,RC3,RC5,RC6,RC7,RC9,RC12,RC14,RC16**

The P-screen photos show the beam oscillating in the vertical plane. This is because at the time of the experiment, the vertical steering was not yet implemented. Moreover, the beam steering and alignment in the straight section is relatively simpler compared to the Y-section, since there are steering elements corresponding to each quadrupole in the straight section of the injector. But by design, as mentioned in the earlier chapter, YQ and PD (Pulsed dipole) are required to bend the beam by  $10^\circ$  degrees. Since YQ is a bending and a focusing magnet (dual function magnet), the injection into YQ is offset by SD6. Moreover, the Y-section is not shielded from the earth's magnetic field. These make injection and steering through Y-section a bit difficult.

A scheme of injection (Collins) was suggested [33], wherein the YQ and QR1 magnets were switched off. The Collins injection scheme made the pulsed dipole do the bending and made the steering through Y-section simpler, but it also changed the matching solution and a new steering solution had to be found. Further discussion about Collins scheme and its comparison with the regular edge injection is described in the Appendix.

The beam size measurement of the 0.55 mA, 5.5 $\mu$ m beam is shown in the Fig below:

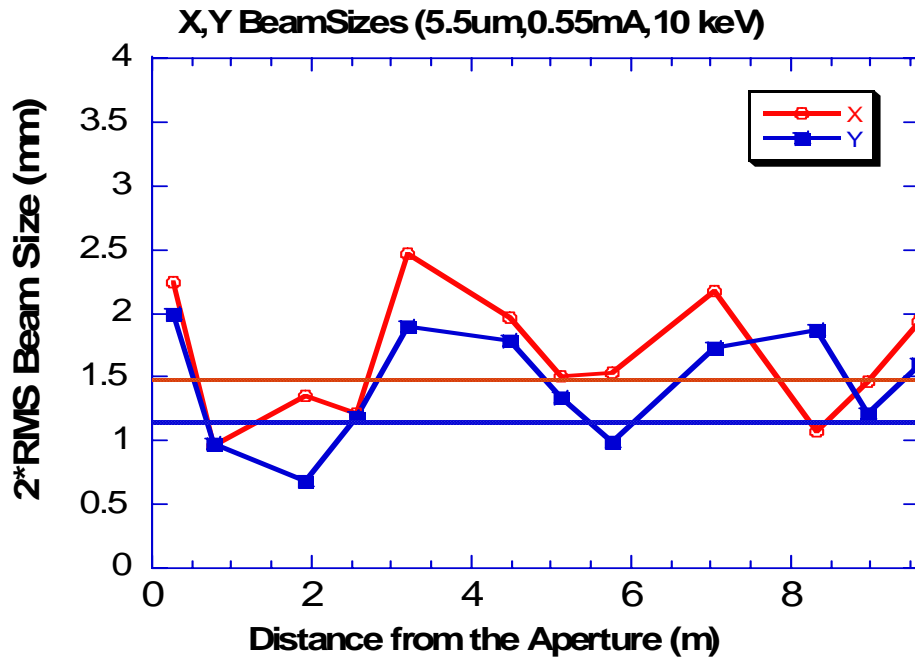


Figure 17 Experimental beam sizes Vs Expected beam sizes for the pencil beam

As it can be seen, the beam is not perfectly matched. The mismatch is mainly due to the uncertainty in the initial beam size, slope of the emittance dominated beam, errors in the solenoid, and the injection offset in the Y-section. Other factors like skew quadrupoles, variations in the beam current, emittance can also contribute to the

mismatch oscillations. A Monte-Carlo analysis of the errors due to these parameters has been systematically studied by [10].

#### 4.2.1.2 Multi-turn experiment

Instead of the standard response measurements like the measurement of beam position in the BPM, a new control algorithm based on Singular Value Decomposition (SVD) was implemented both in the matching section and in the Y-injection section. After calculating the response/sensitivity matrix at all the beam position monitors (BPM) for both the horizontal and vertical correctors, the necessary corrections were applied to the center the beam in the quadrupoles. In addition, the Helmholtz coils that cancel out the horizontal component of the earth's magnetic field are switched on. Under these conditions, multi-turn operation was achieved. The BPM signals from RC2 are shown below:

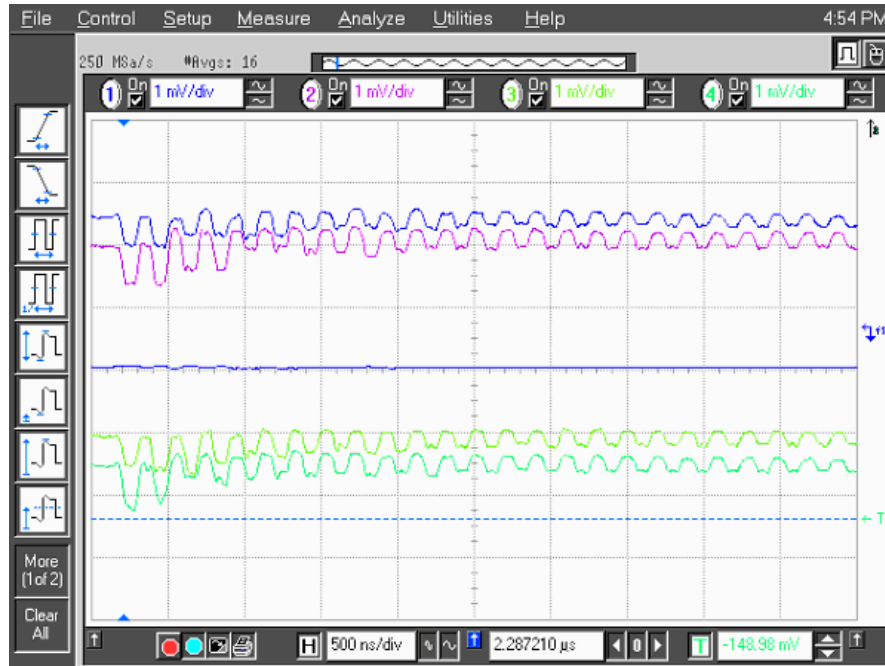


**Figure 18 Multi turn BPM signal output from RC2- More than 100 turns**

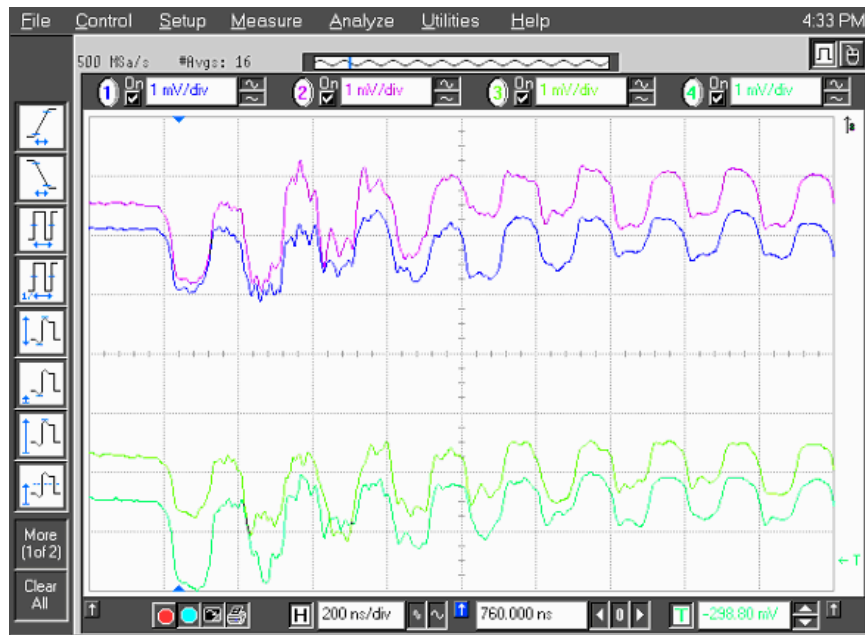


**Figure 19: BPM Signal showing current loss after third turn and stabilizes thereafter**

As the oscilloscope output suggests, there is some current loss after the second turn, but the beam then propagates without any further loss for over 100 turns.

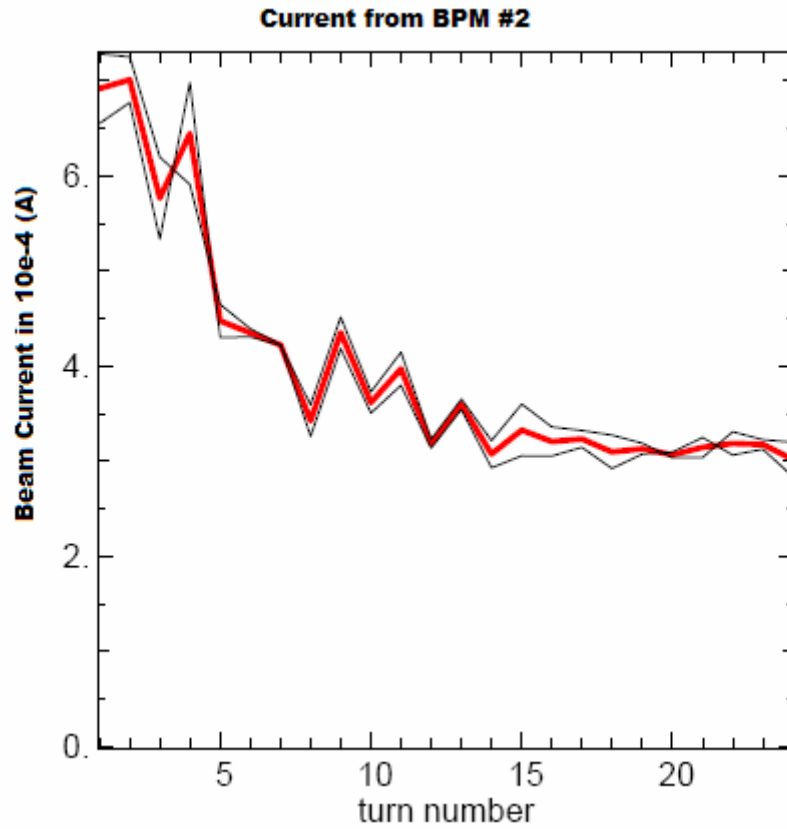


**Figure 20** Beam current for the pencil beam Vs turn number. The thin black lines indicate the error bars in the measurement.

The following table summarizes the results of the calculations based on the experimental results using estimated emittance

**Table 4** Parameters for multi-turn for emittance dominated beam

Phase	Beam Current (mA)	Emittance ( $\mu\text{m}$ )	$\chi$	$v/v_0$	$\Delta v$
Injected	0.69	5.6	0.20	0.89	0.8
After 25 turns	0.3	4.6	0.12	0.94	0.45

### 4.3 Conclusion

The low current, emittance dominated beam has been successfully transported over 100 turns, though with some current loss. This has been largely due to the good matching solution and very good steering solution through the Y-injection line and throughout the ring. The Laslett tune shift of 0.25 has been exceeded by a significant margin. In this chapter, we have demonstrated the systematic way of obtaining the matching solution for multi-turn operation. A good matching solution is of crucial importance for multi-turn operation.



## Chapter 5: Matching of the high current beam

### 5.1 Introduction

In this chapter, the matching of the high current beam in UMER is discussed along with the theory, calculation and experiments. Through proper matching and steering, multi-turn operation of the high current beam has been achieved. The high current beam has appreciable longitudinal and transverse space charge and hence the number of turns achieved is less compared to the low current beam.

### 5.2 Matching of the high current beam in UMER

The high current beam, measures about 23-24mA. The high current beam is obtained by changing the aperture radius to 1.5 mm. The beam emittance of the high current beam is 20 $\mu$ m. This refers to the 4 $\times$  rms beam emittance (unnormalized). The beam radius of the matched pencil beam is around 5 mm.

In the case of a high current beam,  $K= 3.5294e-4$ ,  $\epsilon= 25\mu$ m and  $a= 5$ mm and hence  $Ka^2 > \epsilon^2$ , by a factor of 14, and hence it is a beam in the space charge dominated regime. The tune of the high current beam is 2.06, making the tune shift from the zero-current tune to be 0.27, and hence  $\chi= 0.92$  making it a very intense beam. Transporting an intense beam is one of the primary objectives of UMER. A study of space charge physics requires a well-matched beam to work with.

## 5.2.1 Computer Simulation

### 5.2.2.1 Matching FODO lattice

The matching calculation starts from the periodic FODO lattice.

Basically, a computer code solves the K-V envelope equation for different initial conditions until

$$X(z+S)=X(z), Y(z+S)=Y(z), X'(z+S)=X'(z), Y'(z+S)=Y'(z),$$

where S is the lattice period of 32 cm. The following figure illustrates the same using Trace3D.

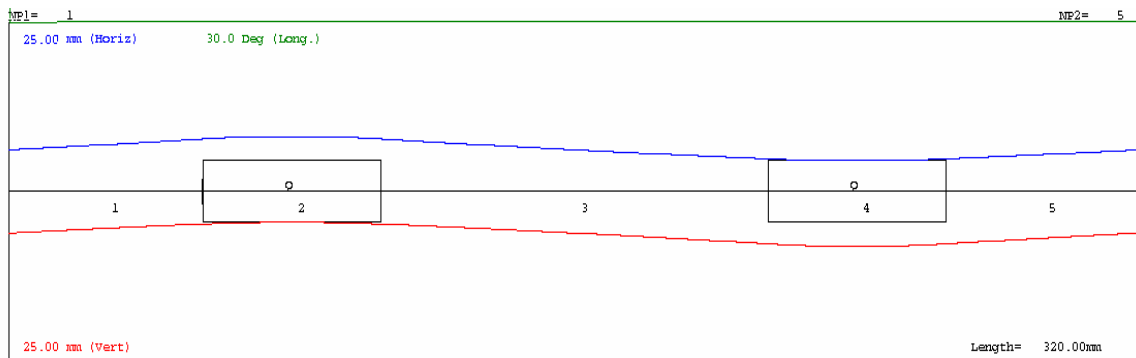


**Figure 21 FODO Matching in TRACE3-D for high current (23.5 mA) beam**

From the above simulation, we can also calculate the expected beam size at the phosphor screen. For the pencil beam  $X= 5.9$  mm, and  $Y = 4.7$  mm. It is seen that the beam size in x-plane is larger than in the y-plane and hence we should expect to see an elliptical beam in every phosphor screen around the ring. The above calculation in Trace-3D, as described in the earlier chapter, uses a hard-edge model for its magnet profile. SPOT calculations are used to get more accurate result, as SPOT models the magnet using a smooth profile.

### 5.2.2.2 Matching Section

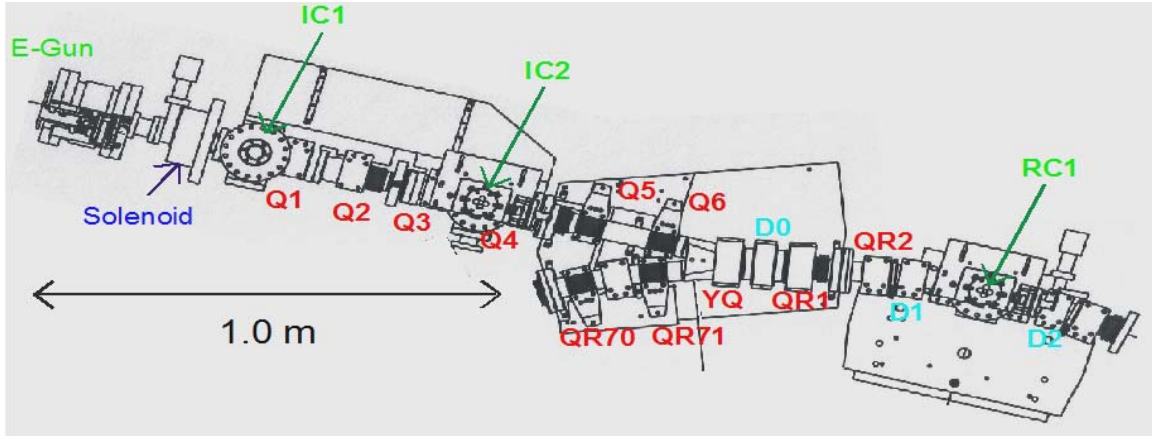


**Figure 22 Top View of the Injection line along with the Y-section and recirculation section**

The above figure depicts the Y-injection section along with the matching section and the ring-section. The matching section consists of solenoid, Q1- Q6 and measures around 1.4 m. YQ, QR1 are big Panofsky magnets and are referred as Y-magnets. QR70, QR71 along with the Y-magnets forms the recirculation part of the ring and Q1, Q2 along with the Y-magnets constitutes the injection part of the ring. Calculating the magnets strength in the matching section is done in stages: First, the ring is solved for recirculation and then solved for injection. This is a crucial design step for multi-turn operation of the machine.

Once the single FODO lattice is run, the necessary target state to be matched becomes available. First, the recirculation section constituting QR71, YQ, QR1, QR2 is matched to get the current settings to match onto the FODO lattice. After this step, the current in YQ, QR1 and QR2 is fixed to the calculated value in the subsequent steps.

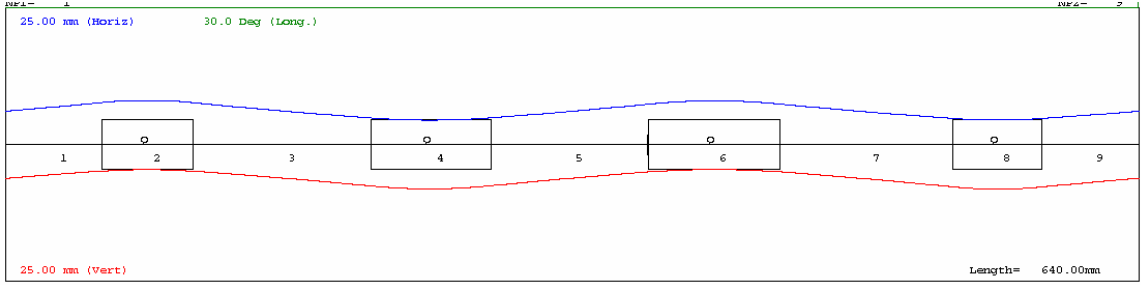


**Figure 23 Multi turn recirculation matching for 23mA beam**

Now, once the values necessary for YQ, QR1 and QR2 is found out, the injector section from solenoid to Q6 is run through the matching program to yield the necessary target state at the FODO Lattice. Note during this step, YQ, QR1 and QR2 is fixed. The intense beam had a comparatively quicker convergence for the matching solution.

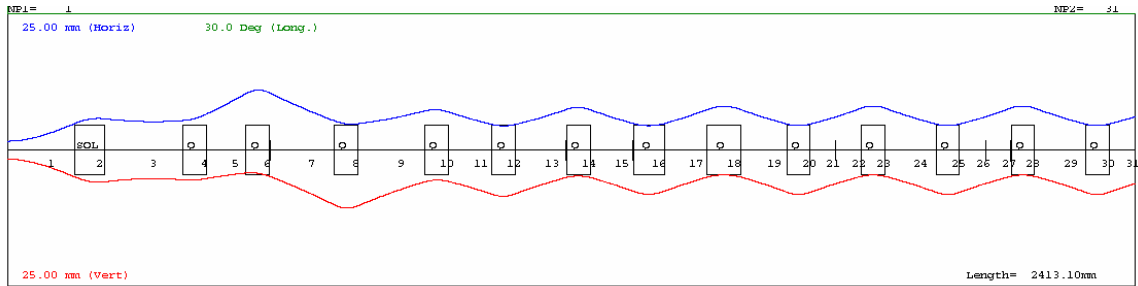


**Figure 24 Injection line matching for 23mA beam**

The values of the injector section settings and the FODO lattice settings for the transport of 23.5 mA beam current and 20 $\mu$ m emittance are tabulated in the table below:

**Table 5 Calculated quadrupole settings for the 23.5mA beam with 20  $\mu$ m**

<b>Magnet</b>	<b>Position (cm)</b>	<b>Current(A)</b>
Solenoid	17.5	5.5
Q1	40.0	1.27
Q2	53.5	2.17
Q3	72.41	1.99
Q4	91.79	1.88
Q5	106.15	1.99
Q6	122.14	2.14
YQ	137.31	5.41
QR1	153.31	5.50
QR2	169.31	1.91
QR3-QR69	185.31[+16 for every quad]	1.88
QR70	1257.31	2.11
QR71	1273.31	2.14

### 5.2.2.3 Empirical Matching

The 23.5mA beam is highly space charge dominated and hence the values calculated from Trace3-D cannot be used in the experiment directly. This is due to the sensitivity of space charge in bends, magnetic profile, etc. The values from TRACE3-D are fed into a WARP deck and then the beam is empirically matched inside WARP. The values calculated by WARP are then used in the experiment. The variation in the beam sizes before and after empirical matching is shown in the figure below.

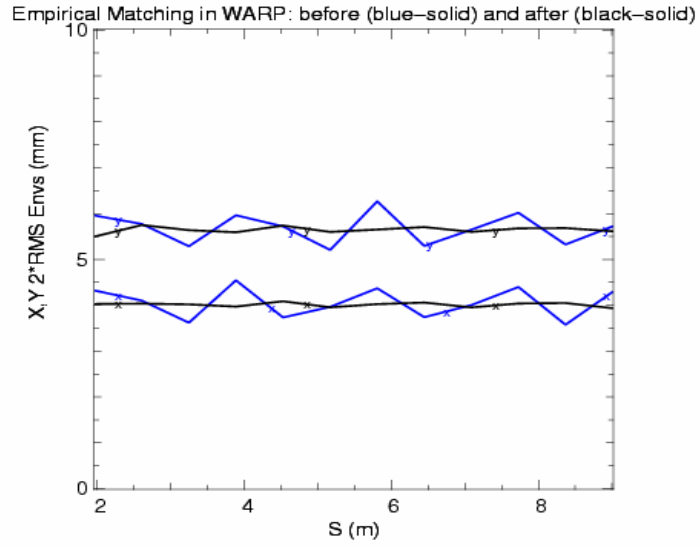


**Figure 25 Empirical matching of 23mA beam in WARP (BLUE- Before: BLACK-After)**

### 5.2.3 Experiment

#### 5.2.3.1 Single Turn Experiment

All the quadrupoles, dipoles and the pulsed elements are set to the required current values using the LabView interface. Phosphor screen photos of a 10 keV, 23.5mA, 100ns beam is shown below:

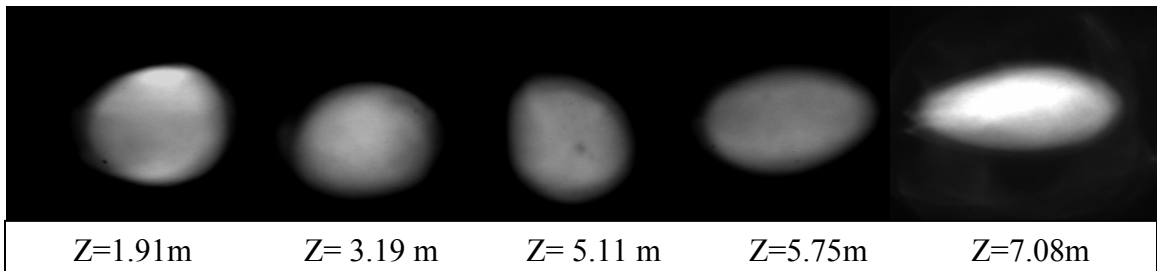


**Figure 26 Phosphor screen output of the 23mA beam**

The beam size measurement of the 23.5mA, 20 $\mu$ m beam is shown in the Fig below:

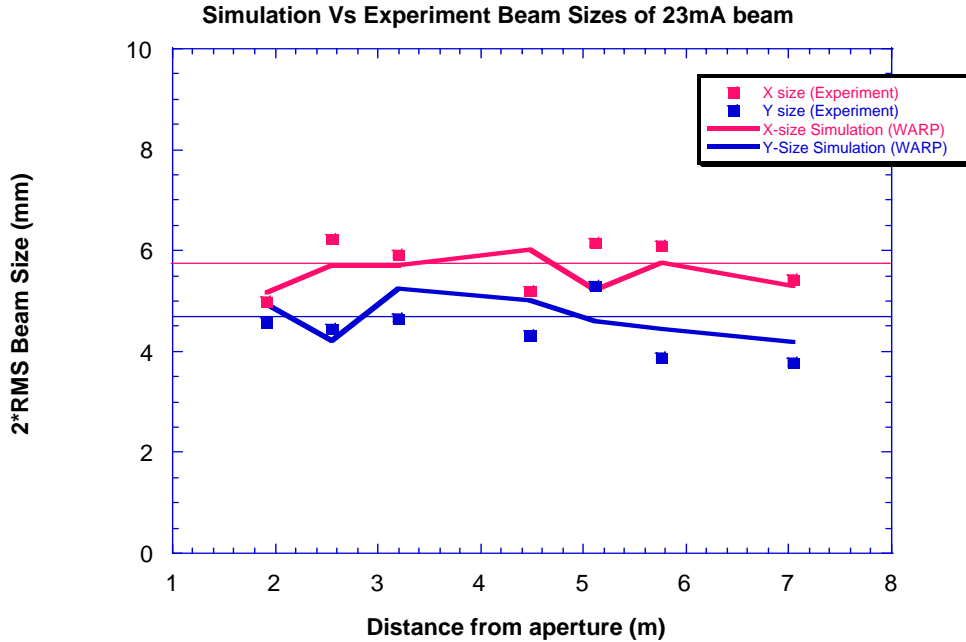


**Figure 27 Measured beam sizes Vs expected beam size of the 23mA beam**

As it can be seen, the beam is not perfectly matched. The mismatch is mainly due to the nonlinear space charge forces, uncertainty in the initial beam size, slope of the emittance dominated beam, errors in the solenoid, and the injection offset in the Y-section. Other factors like skew quadrupoles, variations in the beam current, emittances can also contribute to the mismatch oscillations.

### 5.2.3.2 Multi-turn experiment

A control algorithm based on Singular Value Decomposition (SVD) was implemented both in the matching section and in the Y-injection section. After calculating the response/sensitivity matrix at all the BPMs for both the horizontal and

vertical correctors, the necessary corrections were applied to the center the beam in the quadrupoles.

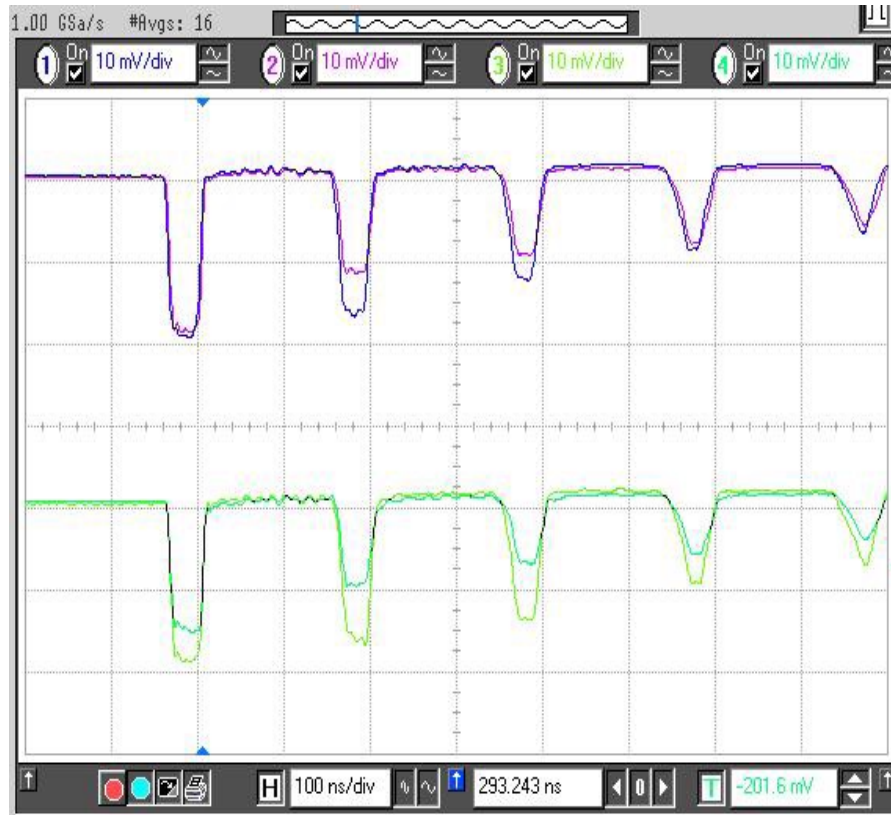


**Figure 28 Output of the BPM signal showing multi turn operation of the 23mA beam**

As the oscilloscope output suggests, the beam continuously loses current on every turn and goes up to 10 turns. The following table summarizes the results of the recent calculations based on the experimental results using estimated emittance

**Table 6 Parameters for multi-turn for a intense beam (23.5 mA)**

Phase	Beam Current (mA)	Emittance ( $\mu\text{m}$ )	$\chi$	$v/v_0$	$\Delta v$
Injected	18.6mA	24	0.7	0.55	3.3
After 25 turns	3.6	10-25	0.48-0.24	0.72-0.87	2.0-0.9



### 5.3 Conclusion

The high current, space dominated beam has been successfully transported over 10 turns, with appreciable current loss. This has been largely due to the good matching solution and very good steering solution through the Y-injection line and throughout the ring. In this chapter, we have demonstrated the systematic way of obtaining the matching solution for an intense beam. A good matching solution is of crucial importance for multi-turn operation.

## Chapter 6: Conclusion

One of the commissioning goals of UMER is to inject a low-current beam and circulate the beam for more than 100 turns. As shown in this thesis work, the goal has been achieved with very little beam current loss. Beam matching was a crucial part of the multi-turn beam transport experiment in UMER. The importance of using appropriate matching codes depending on the problem to be solved was emphasized and elaborated with description of the codes employed in UMER. Matching of an intense, space-charge dominated beam was also described along with the experimental results. Matching the intense beam required using PIC simulation codes like WARP for accurately modeling the space charge effects inside the beam and the beam propagation through the Y-magnets. The thesis concluded with multi-turn experiments on the intense beam.

### 6.1 Suggestions for future work

Multi-turn operation in UMER has been achieved. Now, in order to keep track of the beam size through many turns, a non-interceptive beam size monitor becomes very important. This will make empirical matching over several turns possible and hence the number of turns can be increased. A method suggested by [37] to measure the second moment data from the beam position monitor (BPM) is a promising way to

obtain ellipticity of the beam. Another interesting experiment is to measure the tunes in the X and Y plane and look for resonance crossing and Montague resonance. [38]

## Appendix – Collins Injection

As mentioned in the thesis, another interesting scheme of injection called Collins injection was tested during the work. In Collins scheme of injection, the Y-magnets, YQ and QR1 are turned off. This was done to uncouple bending and focusing done by the YQ magnet. Since the YQ magnet was turned off, the pulsed dipole (PD) had to do the complete  $10^\circ$  bend. Hence, the current on the pulsed dipole increases. Collins injection makes the steering much simpler compared to the classic edge injection. But one of the issues with the Collins scheme is the large envelope excursion, which becomes important in the case of the intense 23mA beam. The image forces takes over the beam and hence matching and steering the beam becomes hard. The following table mentions the pros and cons of the Collins and Classic (Edge injection) schemes.

**Table 7 Comparison between the Classic (Edge) Injection Vs Collins Injection**

Scheme	Dipole peak current on injection/recirculation	Dipole peak current on circulation	Pros	Cons
Classic (With Earth Field)	27.5 A	14 A	YQ Quad helps in bending	Injection angle and Matching are coupled
Collins (With Earth Field)	36-38 A	20 A	No injection angle through YQ	Large envelope oscillation, so for higher beam currents, image forces becomes a problem

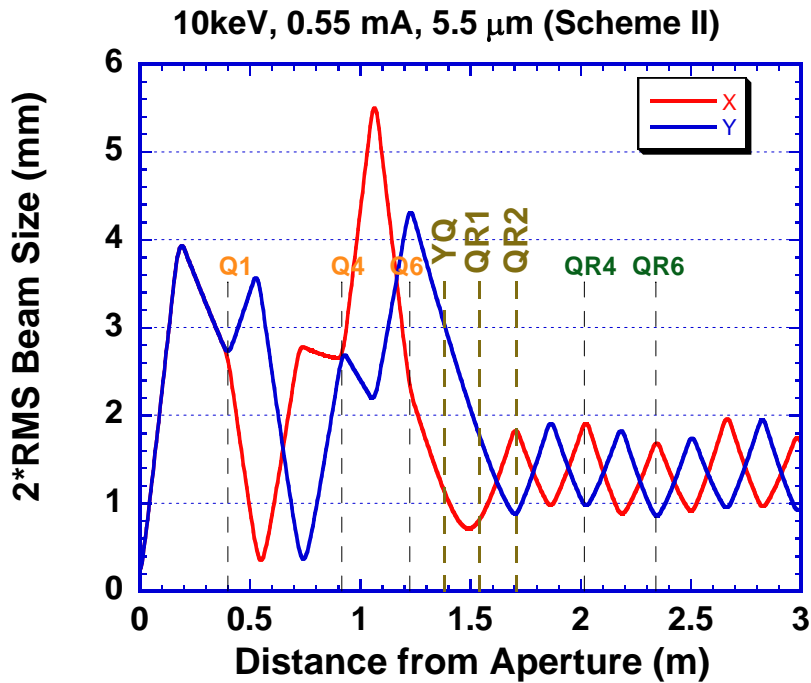


**Figure 29 Simulation of Collins injection scheme for the low current beam**

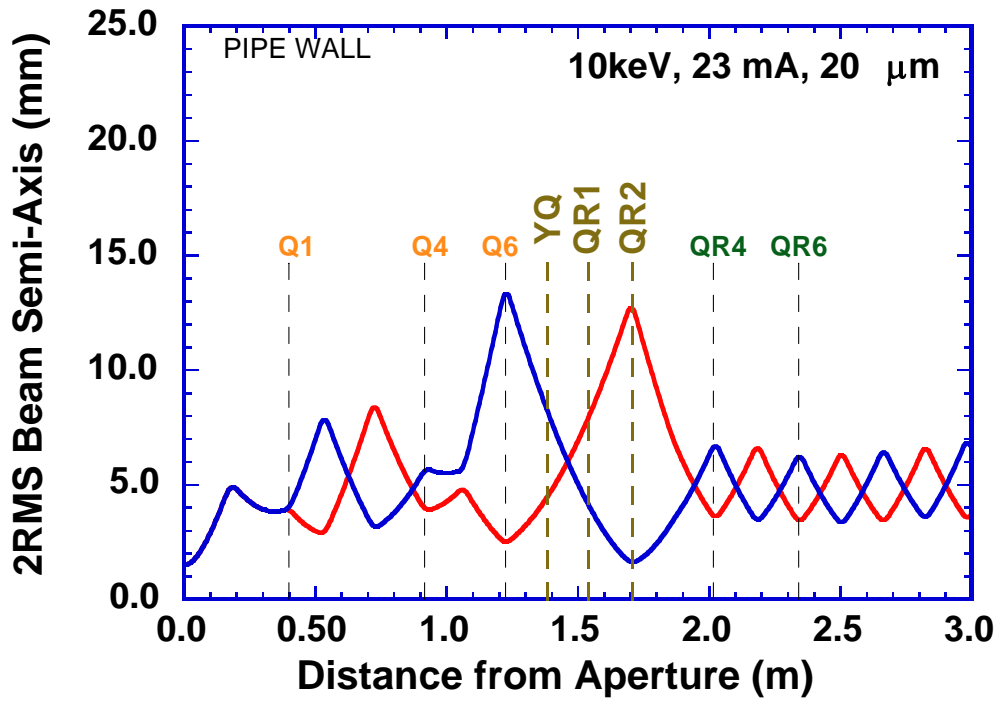


Figure 30 Collins injection scheme for the high current beam showing large envelope excursion

## Bibliography

- [1] T.P.Wangler, K.R.Crandall, R.Ryne and T.S.Wang, "Particle-core model for transverse dynamics of beam halo", Phys. Rev. ST Accel. Beams 1,084201 (1998).
- [2] Robert L. Gluckstern, "Analytic Model for Halo Formation in High Current Linacs", Phys. Rev. Lett. 73, 1247 (1994)
- [3] M.Reiser, Theory and Design of Charged-Particle Beams, WILEY-VCH Verlag GmbH & Co. KGaA, Weinheim (2004)
- [4] M.Reiser, C.R.Chang, D.Kehne, K.Low, T.Shea, H.Rudd, and I.Haber, "Emittance Growth and Image Formation in a Nonuniform Space-Charge-Dominated Electron Beam", Phys.Rev.Letter. 61, 2933 (1988)
- [5] M. J. Syphers, "Injection Mismatch and Phase Space Dilution," Fermilab FN-458, June 1987.
- [6] S. Bernal, P. Chin, R. Kishek, Y. Li, M. Reiser, J.G. Wang, T. Godlove, and I. Haber, "Transport of a space-charge dominated electron beam in a short-quadrupole channel," Physical Review Special Topics - Accelerators & Beams 1, 044202 (1998).

[7] Chris Allen, Ph.D. Thesis, Department of Electrical Engineering, University of Maryland, College Park, 1996

[8] Hui Li, Ph.D Thesis, Department of Electrical Engineering , University of Maryland ,College Park, 2004

[9] H. Li, S. Bernal, T. Godlove, Y. Huo, R.A. Kishek, I. Haber, B. Quinn, M. Walter, Y. Zou, M. Reiser, and P.G. O'Shea, "Beam Control and Matching for the Transport of Intense Beams," Nuclear Instruments and Methods A 544, 367-373 (2005).

[10] S. Bernal, H. Li, R.A. Kishek, B. Quinn, M. Walter, M. Reiser, P.G. O'Shea, and C.K. Allen, "Fixed-Geometry RMS Envelope Matching of Electron Beams from 'Zero' Current to Extreme Space-Charge," Physical Review Special Topics - Accelerators & Beams 9, 064202 (2006)

[11] S.Bernal, et. al., "Space charge beam physics research at the University of Maryland Electron Ring (UMER)", Proceedings of Advanced Accelerator Workshop, Lake Geneva, Wisconsin, (2006)

[12] R.A. Kishek, et.al., "HIF Research on the University of Maryland Electron Ring (UMER)," Nuclear Instruments and Methods A 544, 179-186 (2005).



[13] P.G. O'Shea, et. al, "Intense Beam Experiments at the University of Maryland Electron Ring," Proceedings of the Workshop on Advanced Accelerator Concepts, Mandalay Beach, Oxnard, CA, June 2002 (2002).

[14] M. Reiser, et. al, "The Maryland Electron Ring for Investigating Space-Charge Dominated Beams in a Circular FODO System," Proceedings of the 1999 IEEE Particle Accelerator Conference, New York City, NY, 234 (1999).

[15] R. A. Kishek et al, "PIC code simulations of collective effects in the space charge-dominated beam of the University of Maryland Electron Ring (UMER) ", Proceedings of the 1999 Particle Accelerator Conference, New York, 1999

[16] I. Haber, S. Bernal, R.A. Kishek, P.G. O'Shea, M. Reiser, Y. Zou, A. Friedman, D.P. Grote, and J.-L. Vay, "Computer Simulation of the UMER Gridded Gun," Proceedings of the 2005 IEEE Particle Accelerator Conference, Knoxville, TN, ed. C. Horak, IEEE Cat. No. 05CH37623C, 2908 (2005).

[17] B. Quinn, et. al., "Overview of Electrical Systems for the University of Maryland Electron Ring (UMER)," Proceedings of the 2005 IEEE Particle Accelerator Conference, Knoxville, TN, ed. C. Horak, IEEE Cat. No. 05CH37623C, 3988 (2005).

[18] B. Quinn, et. al., "Design and Calibration of a Fast Beam Position Monitor," Proceedings of the 2003 IEEE Particle Accelerator Conference, Portland, OR, edited by J. Chew, P. Lucas and S. Webber, IEEE Cat. No. 03CH37423C, 2571 (2003).

[19] M. Walter, et. al , "Electro-mechanical Design for Injection in the University of Maryland Electron Ring," Proceedings of the 2003 IEEE Particle Accelerator Conference, Portland, OR, edited by J. Chew, P. Lucas and S. Webber, IEEE Cat. No. 03CH37423C, 1673 (2003).

[20] G.Bai, Master thesis, "Modeling and Experiments on Injection into University of Maryland Electron Ring", Univ. of Maryland, College Park, 2005

[21] W.W. Zhang, et. al, "Design and Field measurement of Printed-Circuit Quadrupoles and Dipoles", Phys. Rev. ST. Accel. Beams 3, 122401, 2000.

[22] H. Li, Master thesis, "Printed-Circuit Magnets System for University of Maryland Electron Ring", Univ. of Maryland, College Park, 2001.

[23] M. Holloway, T. F. Godlove, B. Quinn, M. Reiser, and P.G. O'Shea, "Injector Electronics for Multi-turn Operation of the University of Maryland Electron Ring (UMER)," Proceedings of the 2005 IEEE Particle Accelerator Conference, Knoxville, TN, ed. C. Horak, IEEE Cat. No. 05CH37623C, 3952 (2005).

[24] [www.ni.com/labview](http://www.ni.com/labview).

[25] An operating system for Intel-based and other PCs that is a derivative of Unix and available as freeware

[26] M.Walter, et. al, Beam Control and Steering in University of Maryland Electron Ring , Proceedings of Advanced Accelerator Workshop, Lake Geneva, Wisconsin, (2006).

[27] SPOT contains a detailed manual. Contact [sabern@glue.umd.edu](mailto:sabern@glue.umd.edu)

[28] C.K. Allen, S.K. Guharay, M.Reiser, "Optimal transport of low energy particle beams ", Proceedings of the Particle Accelerator Conference, 1995, Dallas, TX, USA, Vol.4, pp.2324-2326

[29] PBO-Lab is a GUI for Trace 3-D software distributed by AccelSoft & G.H.Gillespie Associates, Inc. available for Windows

[30] Trace 3-D documentation available at <http://laacg1.lanl.gov/laacg/services/traceman.pdf>

[31] A. Friedman, D. P. Grote, and I. Haber, "Three-dimensional particle simulation of heavy-ion fusion beams," Phys. Fluids B 4, 2203 (1992).

[32] D. P. Grote, A. Friedman, I. Haber, "Methods used in WARP3d, a Three-Dimensional PIC/Accelerator Code", Proceedings of the 1996 Computational Accelerator Physics Conference, AIP Conference Proceedings 391, p. 51.

[33] MATLAB Version 7.0, The MathWorks Inc.,

[34] Coleman, T.F. and Y. Li, "On the Convergence of Reflective Newton Methods for Large-Scale Nonlinear Minimization Subject to Bounds," Mathematical Programming, Vol. 67, Number 2, pp. 189-224, 1994.

[35] Coleman, T.F. and Y. Li, "An Interior, Trust Region Approach for Nonlinear Minimization Subject to Bounds," SIAM Journal on Optimization, Vol. 6, pp. 418-445, 1996.

[36] Jayakar Thangaraj, et. al. , " Beam Injection and Matching in the University of Maryland Electron Ring" , Proceedings of Advanced Accelerator Workshop, Lake Geneva, Wisconsin, (2006).

[37] Rami Kishek, Private communication

[38] B.W. Montague, CERN-Report No. 68-38, CERN, 1968.